HCP/T2471-21

Industrial Application Fluidized Bed Combustion Category III Indirect Fired Heaters

Quarterly Technical Report No. 7 January-March 1978

July 1978

Prepared for
U.S. Department of Energy
Assistant Secretary for Energy Technology
Division of Power Systems

Under Contract No. EX-76-C-01-2471

Available from:

National Technical Information Service (NTIS)
U.S. Department of Commerce
5285 Port Royal Road
Springfield, Virginia 22161

Price: Printed copy: $5.25
Microfiche: $3.00

HCP/T2471-21
UC-90e

Industrial Application Fluidized Bed Combustion Category III Indirect Fired Heaters

Quarterly Technical Report No. 7 January-March 1978

July 1978

Prepared by
Exxon Research and Engineering Company
Engineering Technology Department
Florham Park, New Jersey

For

U.S. Department of Energy
Assistant Secretary for Energy Technology
Division of Power Systems
Washington, DC 20545

Under Contract No. EX-76-C-01-2471

TABLE OF CONTENTS

LIST OF FIGURES

Nomenclature

A_T - tube cross sectional area

B.E. - bed expansion, equation 7

B.S.V. - bundle space velocity, B.S.V. = $\frac{QH_B}{D_B} \quad \frac{1}{W_B H_B - A_T N_T}$

d_p - average particle diameter

D_B - bed dimension parallel to the horizontal tubes.

Ga - Galileo number, equation 4

g - acceleration due to gravity

g_c - conversion factor

H_B - tube bundle height between top and bottom row tangent lines

H_{mf} - expanded bed depth at minimum fluidization

H_s - static bed depth

H_e - expanded bed depth

N_T - number of tubes in the tube bundle

$\triangle P$ - bed pressure drop

Q - volume flow rate of gas phase

Re_{mf} - particle Reynolds number at minimum fluidization

u - superficial gas velocity

u_{mf} - minimum fluidization velocity

W_B - bed width

Greek Symbols

ϵ - void fraction

ϵ_{mf} - void fraction at minimum fluidization

μ - viscosity of the fluidizing gas

ρg - density of the fluidizing gas

ρp - density of the bed solid particles

ϕ_s - particle sphericity

ABSTRACT

A program is underway to evaluate the technical and economic potential for the application of fluidized bed combustion to refinery and petrochemical plant indirect fired process heaters. The strategy of the program is to build on available boiler oriented FBC technology. Areas common to both steam generating boilers and process heaters will not be intentionally advanced by this program. However, the results of complementary programs in the boiler area will be considered in the assessment of potential heater applications.

Two pertinent areas that are not being addressed in the on-going boiler oriented programs and which are being investigated here concern the effects of larger tube size and hydrocarbon coking. Phase I of the program consists of the design, construction and operation of three laboratory facilities to carry out these studies. Fluidized bed performance studies, including bed mixing and density measurement, have been completed on six alternative tube bundle configurations ranging from 2-inch to 6-inch diameter tubes arranged on nominal 2-diameter, 3-diameter and 4-diameter horizontal spacing. Conductive/convective heat transfer coefficients as a function of tube size, location and surface orientation have also been obtained on these same bundle configurations and on isolated single tubes. Finally, evaluations have been made on the effect of altering the tube-to-grid dimensions and of operating with limestone beds of different particle size distributions.

A Process Stream Coking Test Unit has been commissioned and is being used to study the parameters affecting coke laydown on the internal surfaces of hydrocarbon containing tubes under conditions of high temperature and heat transfer rate.

Design and early procurement activities are underway for the third laboratory facility which will be a "hot" coal fired fluidized bed combustor. This facility will be used to study overall heat transfer coefficients and combustion performance.

1. Objectives and Scope of Work

The purpose of this program is to extend the state-of-the-art of fluidized bed coal combustion, which at present, addresses the generation of steam to applications where oil passing through immersed tubes in the bed will receive heat and be heated to a required condition. This purpose will be achieved by the successful completion of the following program objectives:

a. To conduct an R&D program necessary to provide the engineering data and know-how for designing a fluidized bed process heater.

b. To conduct an economic analysis necessary to evaluate the economic attractiveness of fluidized bed combustion for indirect fired process heater applications.

c. To demonstrate the operation of a coal fired fluidized bed heater in an actual refinery environment for an extended period of time.

d. To prepare a complete Design Specification and Control Cost Estimate for a commercial sized fluidized bed coal fired process heater.

The basic approach to be followed in pursuing the objectives of this program will be to build on the fluidized bed technology that is now available and under development by others in the related areas of fluidized bed boiler applications. Effort in this program will be concentrated on doing the incremental work necessary to extrapolate the boiler oriented technology to refinery and petrochemical plant type indirect fired process heaters. The areas of technology common to both steam generating boilers and process heaters will not intentionally be advanced by this program. However, the state-of-the-art and the results of complementary programs in the boiler area will be used in the overall technical and economic assessment of potential fluidized bed process heater applications.

The two principal areas of technology that have been identified as being peculiar to process heater applications and which are not being addressed in the on-going boiler orientated programs concern the effects of tube size and hydrocarbon coking. These two areas will be investigated in this program.

Indirect fired process heater tubes are conventionally two to five times larger in diameter than boiler tubes. A typical crude oil heater, for example, may have a multitude of 4" to 8" diameter tubes in the heat pick-up zones as contrasted to the 1" to 2" diameter tubes normally used in steam boilers. The effect that these larger tubes will have on fluidization characteristics and definition of the optimum or acceptable configuration of a tube bundle immersed within a fluidized bed must be investigated.

Similarly, the parameters affecting hydrocarbon coking must be investigated. When heating a hydrocarbon to 600°F+ (as required for separation by distillation or other typical processes) some degradation of the oil and coke laydown on the inside tube wall is unavoidable. The rate of coke laydown is affected primarily by the temperature of the hydrocarbon film on the inside wall of the tubes. This film temperature, in turn, is a function of several parameters relating inside film coefficient and heat transfer rate. Both overall average and localized conditions within the heat transfer zone must be examined.

The effects of tube size and coking described above will be investigated during the initial laboratory R&D phase of the program. This will be accomplished through the design, fabrication and operation of three separate laboratory test units. These units are designated as follows:

a. Two-Dimensional Flow Visualization Unit

b. Process Stream Coking Unit

c. High Temperature Heat Flux Unit

Other portions of the Phase I effort involve economic and operability evaluations of the technology and design of the Phase II Demonstration Unit followed by the Design Specification and Control Cost Estimate for a commercial-sized FBC process heater.

If, at the conclusion of Phase I, the technical and economic assessment of the data indicate favorable commercial potential, the program will be advanced to the demonstration phase. This will involve the installation of a 10-15 MBtu/Hr coal fired fluidized bed process heater in an Exxon refinery and its operation for a sufficient period of time to obtain the engineering data necessary to design a commercial sized facility.

2. Summary of Progress to Date

The Program is structured into 10 tasks or cost centers which are being used to monitor and report the progress of work. The overall schedule and identification of tasks are shown in the Milestone Schedule Chart included here as Figure 1.

The first major laboratory task, namely, the Two-Dimensional Flow Visualization Study, has been completed. This study evaluated the effect on fluidization performance and heat transfer characteristics when an array of relatively large diameter tubes was immersed in a fluidized bed of limestone. Alternative configurations of tubes up to 6 inches in diameter and spaced on 2 to 4 tube diameter center-to-center spacing were investigated. The studies defined the range of acceptable tube bundle configurations that might be used in commercial process heater applications. Engineering data on fluidization parameters and conductive/convective heat transfer patterns were obtained.

All single tube and tube bundle data were reported in previous Quarterly Technical Reports. The remaining unreported task data on the effects of altering the tube-to-grid spacing and of changing the bed particle size distribution are covered in this report.

The Process Stream Coking Test Unit was commissioned during this reporting period and a hot calibration run was successfully completed. The unit is now out of service due to a scheduled maintenance turnaround of the associated refinery Atmospheric Distillation Unit which provides crude oil feed to the test unit. Program testing will be resumed during May.

The vendors' detailed construction drawings have been approved for the Heat Flux Test Unit. Other procurement activities are continuing.

3. Discussion of Technical Progress

3.1 Two-Dimensional Flow Visualization Studies

3.1.1 Background Information

The Flow Visualization studies were carried out in a two-dimensional atmospheric pressure, transparent fluidized bed chamber. The unit was approximately 1 ft. in depth by 7.5 ft. wide by 12 ft. high (see Figure 2). The facility was designed to accommodate a range of tube bundles assembled from tubes up to 6 inches in diameter and arranged on spacings up to 4 tube diameters on center.

Tube bundles were immersed in the bed and the effect on fluidization of these relatively large tubes was determined through a systematic study of the parameters of tube diameter, tube-to-tube spacing, tube-to-grid spacing and tube orientation. Other variables such as bed particle size, fluidization velocity, grid location and bed pressure drop were also examined although these were of secondary interest since they are being investigated by other boiler oriented programs.

A discussion of the overall Test Plan for this subtask including a description of the facility and the planned test sequence was included in the Program Quarterly Technical Report No. 1 dated October 19, 1976. The interested reader is referred to that report for more detailed background information.

3.1.2 Status of Work

This program task work is completed. A total of six bundle configurations have been evaluated. These bundles were made up of nominal 2-inch, 4-inch and 6-inch diameter tubes arranged on 2-diameter, 3-diameter and 4-diameter center-to-center horizontal spacing. Two different vertical spacings were also tested. The results of these alternative bundle evaluations on parameters of fluidization velocity, bed mixing and conductive/convective heat transfer were reported in Program Quarterly Technical Report Nos. 5 and 6.

During the current reporting period additional tests were conducted to define the affects of altering the tube-to-grid dimension, changing bed inventory and using bed materials with differing particle size distribution. And finally, all the data obtained during the course of these Flow Visualization studies were used to develop a correlation for predicting expansion of a fluidized bed as a function of fluidization velocity and bundle configuration.

3.1.3 Description and Analysis of Tests

Prior to presenting the results from these tests it will be helpful to describe the tests that were run and the comparisons that will be made. All of these tests were carried out using the 4-inch diameter tubes on 2-diameter equilateral triangular pitch (4"-2DE). Two grid-to-tube spacings were used (18" and 10") and three bed material inventories (18", 10" and 21" above the grid). The various combinations of bundle location and bed loadings are schematically illustrated in Figure 3.

Limestone bed materials of four different size distributions were tested. These are shown in Figure 4. Limestone Blends A and B had identical top sized particles (5600μ) but a modified weight average size while Blend C had a much lower top size (2800μ). Blend D was the 1410μ minus sized particles screened from a combination of the above blends. These four blends are overlapping in size; that is, the distribution of smaller sized particles is nearly identical for all blends while the concentrations of larger particles have been altered. If the 1410μ minus portions of the blends are plotted as in Figure 5 it is seen that the fines distribution for all blends is relatively similar.

The investigation into the effects of particle size on fluidization characteristics as conducted in this series of tests is rather unique. The classical approach in examining particle size effects as investigated by others and in earlier work done in this program has been to test over narrow and discrete particle size ranges. For instance, in Reference (1) the effect of particle size was investigated by looking at 390μ and 1000μ glass beads. Testing with a broad and overlapping particle size blend as done here is more representative of commercial conditions since, regardless of the starting material, an operating bed will always equilibrate to a relatively broad blend because of bed material attrition and agglomeration.

From this series of experiments with varying tube-to-grid spacing, solids loading and bed particle size distribution, a number of useful observations and comparisons can be made. These include:

a. Measured and calculated minimum fluidization velocities as a function of particle size distribution.

b. Predicted expansion of a fluidized bed as a function of fluidization velocity and bundle configuration.

c. Effect of varying bed particle size distribution on heat transfer rates.

d. Effect of varying tube-to-grid spacing on heat transfer rates.

Each of these areas will be discussed in the following paragraphs.

3.1.3.1 Correlation for Minimum Fluidization Velocity

Theoretical predictions and experimental measurements of the minimum fluidization velocity, u_{mf}, are available for fine bed materials within a narrow size range. However, there is little information available for predicting minimum fluidization velocity for large particles or wide blends of particles. Interestingly enough, it is in this region of large blended particles that fluidized bed combustors will operate. Cranfield and Geldart (4), Saxena (2), and Louis (3) are researchers presently contributing to this area of large particle fluidization.

The minimum fluidization velocity has the greatest meaning where a sharp transition from fixed to fluidized bed occurs. In a wide particle size distribution this does not occur; however, it can be demonstrated that u_{mf} is still a useful term.

Ergun Correlation Used

Correlation of the minimum fluidization velocity for particle blends A,B,C and D was attempted using the Ergun (5) correlation as suggested by (2 and 6). At incipient fluidization the pressure drop across the bed is

$$\frac{\Delta P_{mf}\, g_c}{H_{mf}} = \left(1-\epsilon_{mf}\right)\left(\rho_s - \rho_g\right) g \qquad (1)$$

Ergun proposed the correlation for minimum fluidization

$$\frac{\Delta P_{mf}\, g_c}{H_{mf}} = 150 \frac{\left(1-\epsilon_{mf}\right)^2 \mu\, u_{mf}}{\epsilon_{mf}^3 \left(\phi_s \bar{d}_p\right)^2} + 1.75 \frac{\left(1-\epsilon_{mf}\right) \rho_g\, u_{mf}^2}{\epsilon_{mf}^3 \left(\phi_s d_p\right)} \qquad (2)$$

Combining Equations 1 and 2 results in:

$$150 \frac{1-\epsilon_{mf}}{\phi_s^2\, \epsilon_{mf}^3} Re_{pmf} + 1.75 \frac{Re_{pmf}^2}{\phi_s\, \epsilon_{mf}^3} - Ga = 0 \qquad (3)$$

where

$$Ga = \frac{d_p^3 \rho_g \left(\rho_s - \rho_g\right) g}{\mu^2} \qquad Re_{pmf} = \frac{\bar{d}_p \rho_p u_{mf}}{\mu} \qquad (4)$$

Equation 3 is usually difficult to use since neither the sphericity, ϕ_s, nor ϵ_{mf} are known. However, Saxena (2) in measurements of fresh dolomite of an average particle size of 700+μ has determined values for the two important groups in Equation (3). These are:

$$\frac{1 - \epsilon_{mf}}{\phi_s^2 \epsilon_{mf}^3} = 5.9 \qquad \text{and} \qquad \frac{1}{\phi_s \epsilon_{mf}^3} = 10 \qquad (5)$$

with a measured mean sphericity of the dolomite of $\phi_s = 0.8$

Substituting values from Equation 5 into Equation 3 permits a direct solution of u_{mf}:

$$u_{mf} = \frac{\mu}{d_p \rho_g} \left\{ \left[(25.3)^2 + 0.0571 Ga\right]^{1/2} - 25.3 \right\} \qquad (6)$$

The constants in Equation 6 are modified slightly from that proposed in (6). Both Saxena and Wen and Yu, however; recommend use of the weight average particle size in Equation 6.

Experimental vs. Predicted Values for u_{mf}

The observed and predicted minimum fluidization velocities for particle blends A,B,C and D are shown in Figure 6. As can be seen, use of the weight average particle size in Equation 6 results in a severe over prediction of the u_{mf} value. However, when the volume mean particle diameter is used as the correlating particle size, closer agreement between predicted and observed minimum fluidization values result. The volume mean diameter is the dimension of that particle having a volume that is the average of the volumes of all the particles in the sample.

3.1.3.2 Expansion of the Fluidized Bed in the Tube Region

Previous studies (7) have shown that the appropriate parameter to correlate bundle performance is the bundle space velocity (B.S.V.) which represents the integrated average velocity through the bundle region. Therefore, initial attempts were made to correlate bed expansion against the B.S.V. In this case, the bed expansion was defined as the ratio of the expanded bed volume to static volume minus the tube volume covered, or:

$$\text{Bed Expansion} = \text{B.E.} = \frac{H_e\, W_B D_B - (\text{Tube Volume in } H_e)}{H_s\, W_B D_B - (\text{Tube Volume in } H_s)} \quad (7)$$

The bed was assumed to be fully expanded at a bed density of 18 lb/ft^3.

The bed expansions for limestone blends A, B and C appeared to correlate well against the single parameter B.S.V. However, Blend D, which was the finer blend with the larger particles removed, did not follow the same trend. Expansion for Blend D was more rapid than for the three other blends. The expansion data for all four particle blends were the normalized on the basis of minimum fluidization velocity u_{mf}. The resulting correlating plot (B.E. vs BSV/u_{mf}) for all data is shown in Figure 7.

Perhaps it would be instructive to evaluate one bed expansive to clearly define each term. Reference is made to Figure 8a for arithmetic values at 3.9 fps superficial velocity. Complete details on the bundle layout and bundle space velocity factor, B.S.V., can be obtained in Reference (7).

Static Bed Condition

$H_s = 18"$

$D_B = 12"$

$W_B = 90"$

Tube volume in H_s = 1/2 of 11 tubes in first row

$$= 1/2\ (11)\frac{\pi\ (4.5)^2}{4}\ (12) = 1050\ in^3$$

Expanded Bed (up to ρ_{bed} = 18 lb/ft^3)

H_E = 28"

D_B = 12"

W_B = 90"

Tube volume in H_E = 2 rows of tubes covered

$$= (11 + 10)\ \frac{\pi\ (4.5)^2}{4}\ (12) = 4000\ \text{in}^3$$

Velocity Term

Superficial velocity = 3.9 fps

u_{mf} = 2.3 (see Figure 6)

B.S.V. Factor = 1.42 see Reference (7)

$$\frac{\text{B.S.V.}}{u_{mf}} = \frac{(1.42)\ 3.9}{2.3} = 2.48$$

Bed Expansion

$$\text{B.E.} = \frac{28(12)(90) - 40000}{18(12)(90) - 1050} = 1.42$$

Therefore at 3.9 fps the bed of particles consisting of blend A experienced an expansion of 1.42. As can be seen from Figure 8a the bed had expanded and fully covered the tube bundle at 12.1 fps. Therefore, the final density plot at 14.8 fps would not be used in evaluating bed expansion since the bed had expanded through the tube bundle prior to that velocity.

Bed expansion data at 8 and 9.7 fps for 4"-2DE Blend B material (Figure 8b) were not used in developing the correlating plot since bed plugging and reduced circulation of bed material was observed for this condition. Refer to Reference (7) for a complete discussion of this phenomena.

3.1.3.3 Effect of Varying Particle Size Distribution on Heat Transfer Coefficient

The effect of varying particle size on heat transfer coefficient was investigated with the tube-to-grid spacing of 18 inches and solids loading of 18 inches. Particle size distributions A,B,C and D were evaluated. The heat transfer probes used consisted of specially instrumented plexiglas tubes which were installed in the fluidized bed zone of the test unit. Each tube had a 1/4" x 6" x 0.05" thick Nichrome strip imbedded flush with the outside tube surface. These strips were electric resistance heated. One or two 40 BWG iron-constantan loop junction thermocouples were attached to the under surface of the strip. The heat transfer coefficients were determined from power input, strip temperature, strip area and bed temperature measurements, (see reference (7) for a complete description of the probe).

The reduced data in the form of heat transfer coefficients are shown in Appendix I. The row average heat transfer coefficients for rows 1,3, and 5 and the four particle size distributions are shown on Figures 9,10, and 11. The corresponding bed density plots are shown as Figures 8a,b,c, and d.

Row 1 data (Figure 9) represent values for the heat transfer coefficient when the tube is totally within the fluidized bed zone. Several interesting observations can be made. First, the heat transfer coefficients for Blends A,B, and C appear to be similar while D, the finest material, falls well below other data. Particle size distributions A and B have equal top sized material while 30-40% of the bed material in these blends is larger in size than that found in distribution C. The implication is that the larger particles do not contribute significantly to the heat transfer mechanism.

Comparison of Blend D heat transfer data with that of Blends A,B and C; however, shows an interesting result in that at any given B.S.V. the heat transfer coefficient for Blend D is the lowest, yet the particles are the finest. This is an apparent contradiction to the work of others and that reported in (1,8) where smaller particles were shown to have higher heat transfer coefficients than larger particles.

A possible explanation of this seeming contradiction may be suggested by the earlier reported observation that the bed material with the large particles removed (Distribution D) tended to expand more rapidly than the blends containing the large particles. It is hypothesized that as the finer bed expands the bed density is reduced and the frequency of contact between particle and tube wall is correspondingly reduced. With less particle to tube contact it would follow that the heat transfer rate would be lower.

If Figure 9 data are replotted at equal bed expansion (heat transfer coefficient vs. B.S.V./u_{mf}) the data for Blends A,B,C and D all fall nicely on one correlating line. (see Figure 12) The data for rows 3 and 5 are similarly replotted on Figure 13 and 14. Row 3 data (Figure 13) show reasonable consistency with the correlating line shown. Fourteen of the sixteen data points cluster tightly about this line. The remaining two points (distribution B at $BSV/u_{mf} = 4$ and distribution D at $BSV/u_{mf} = 5.8$) display a significant deviation. A review of the experimental technique used to obtain these points and the laboratory data revealed no reason to suspect these points are in error.

Row 5 data (Figure 14) do not display the same degree of consistency as Rows 1 and 3. The data do fall into a $\pm$ 20% band around a correlating line; however, different trends for the data can be observed. Simply compare Distribution B and D data separately and the differences become apparent. This suggests that the correlating parameter (B.S.V./u_{mf}) is not complete in that it cannot account for the various forms of particle activity observed at the top row and the nature of the particle size distribution may have an effect on this free board/splash zone tube.

However, the general implication is that although particle size is an important parameter in determining the heat transfer coefficient in a narrow range distribution it is not as important in a wide blend mixture. As long as the distribution of particles in a blend is continuous the heat transfer coefficient will be controlled by the smaller particles in the blend and will be relatively insensitive to the top sized material or the weight average. Obviously, there is need for further investigations of this finding.

3.1.3.4 Effect of Varying Tube-to-Grid Spacing

The effect of varying the tube center line to grid spacing was investigated in a series of experiments using limestone Blend B. Ten inch and 18 inch tube center line to grid spacings were tested with a bed depth of either 18", 10" or 21" above the grid. The 18" and 10" bed depth corresponded to loading bed material until the level reached the center line of the lowest tube row for the 18" and 10" grid-to-tube bundle locations, respectively. The 21" bed depth case corresponded to a mass inventory of solids equivalent to the 18" case but with the bundle lowered to 10" above the grid location. The 3" increase in bed level resulted from the displacement of solids by the tubes in the bed zone. (Again, refer to Figure 3).

The results of the heat transfer experiments are shown on Figure 15. In both the 10/10 case (10" of material with a 10" grid-to-tube spacing) and the 18/18 case (18" material and 18" grid-to-tube) the row 1 data are directly comparable since the tubes were fully immersed in both cases. The 21/10 case (21" material with 10" grid-to-tube) corresponds to a condition where both rows 1 and 3 were fully immersed at all velocities above minimum fluidization since the static loading of solids was equivalent to the third row bottom tangent line. The density profiles for the 10/10 and 21/10 beds are shown on Figure 17a,b. The density profiles for the 18/18 case are shown on Figure 8b.

As can be seen from the row 1 heat transfer coefficients the heat transfer rates are similar for all three solids loadings and therefore no effect is observed on tube-to-grid spacing. In addition, no significant effect of tube-to-grid spacing was observed on average bed density in this region (Figure 16).

The row 3 heat transfer coefficients for the 10/10 and 18/18 arrangements are also quite similar. These data again show no effect of grid to tube spacing. This is especially true above a BSV of 9 fps where the limestone particles are completely fluidized and the bed fully expanded. Below 9 fps the trend in the data suggests a possible dependence on bed expansion because of the observed higher heat transfer coefficients in the 18/18 case. The 18/18 situation requires a smaller percentage of bed expansion prior to inundating the third row tubes than the 10/10 case.

The two row 3 data points for the 21/10 case are also interesting. At the higher velocity the 21/10 heat transfer coefficient is nearly identical to that measured for the 18/18 and 10/10 arrangements. In this velocity range the limestone is fully fluidized. Again, no dependence on the grid to tube spacing or solids loading is observed. At the lower 21/10 velocity a significant deviation from the 10/10 and 18/18 heat transfer coefficients is observed. This can possibly be attributed to bed expansion. At this low velocity and the lower solids loadings the bed has not expanded to the point where this tube is fully immersed in the fluidized bed. In the 21/10 case the initial solids level is equal to the lower tangent for the third row tube. Therefore, any bed expansion results in this tube being fully immersed in the fluidized bed. This suggests that the 21/10 low velocity data should be more comparable to the row 1 data, which it is.

The row 5 heat transfer data clearly show a dependence on bed expansion. Both the 18/18 and 21/10 beds require smaller bed expansion prior to placing solids on the top row than that required of the 10/10. The 10/10 heat transfer coefficients are obviously the lowest.

3.1.4 Summary Conclusions and Observations

From an analysis of the data gathered in this series of tests the general observations and conclusions can be summarized as follows:

1. The prediction of minimum fluidization velocity for a blend of particles with a wide size distribution should be based on the volume average particle size of the blend rather than on the weight average particle size.

2. The bed expansion through the tube bundle region can be expressed as a simple function of bundle space velocity and minimum fluidization velocity.

3. In a wide blend bed material, overall bed particle size distribution is not an important parameter in determining heat transfer coefficients. Heat transfer performance is predominantly determined by the finer particles in the blend so long as the distribution of particles is reasonably continuous. However, the presence of larger particles tends to suppress bed expansion such that overall heat transfer coefficients may be higher for a wide blend particle distribution than for a narrow blend of the finer portion of the same materials. Heat transfer rate for the range of particle blends tested correlates well with the parameter of bundle space velocity divided by minimum fluidization velocity, B.S.V./u_{mf}.

3.2 Process Stream Coking Studies

3.2.1 Background Information

The Process Stream Coking Studies are designed to determine what effect the high heat flux rates available in a fluidized bed combustor will have on the coking rate of a hydrocarbon stream and if these coking rates can be controlled within an acceptable range of operations. More specifically, they will establish a relative rate of carbon or coke deposition on the inside wall of a hydrocarbon containing tube as a function of bulk temperature, heat flux, mass velocity and inside film temperature.

The test facility that has been built to carry out these studies has been installed at Exxon's Bayway Refinery, Linden, N.J. The unit consists of four heat exchangers, each heated by an electric radiant heater. Each exchanger is a single 0.6 inch I.D. x 9 ft. long (heated length) stainless steel tube. The basic scheme is to pass a stream of virgin crude oil through each of the four exchangers. Total unit throughput is approximately 900 Bbl/Day.

Each exchanger is exposed to a different combination of process conditions (mass flow, bulk temperature and heat flux) and each is carefully monitored for indications of coke deposition on the inside surface of the exchanger tube. In this way, comparative coking rates as a function of the varying process parameters can be determined.

A detailed description of the facility including a discussion of the planned test matrix and basis to be used for analysis of data is given in the Quarterly Technical Report No. 2 dated January 26, 1977. The reader is referred to that report for more detailed background information.

3.2.2 Hot Calibration Run Completed

The Process Stream Coking Test Unit was put into operation during this reporting period. After a period of circulation and flushing with hot crude oil, the electric heaters were activated on March 7th. This was the start of an 8-day continuous run which was used to hot calibrate all instruments and to generate sufficient data to check the mass and energy balances on the unit.

The general procedure used was to gradually increase the bulk crude inlet temperature and/or flux rate on each of the heaters to successively higher plateaus over a period of days. At each plateau the unit was allowed to come to equilibrium and a set of data obtained before moving to the next higher severity of operation. End-of-run conditions reached were 640°F crude inlet temperature and a nominal 45,000 Btu/hr ft^2 flux rate. These conditions do not represent the most severe included in the planned test matrix but do provide sufficient information to establish the baseline operation of the unit.

The calibration run also identified a number of equipment and instrumentation deficiencies that required correction before the first planned test could be started. The more pertinent items included the following:

1. The Robicon power controllers for the individual electric heaters have been a continual source of trouble and had to be returned to the supplier for service. One of the four units was not received in time to be reinstalled for the calibration run. However, all units are now installed and appear to be functioning satisfactorily.

2. Three of the system safety valves released during startup and did not reseat properly. This required operating at a system pressure about 70 psi below that planned. The valves were removed and reset at the end of the run and reinstalled.

3. The Sundyne high pressure booster pump is designed to operate with a buffer fluid between the seal oil and crude oil sides of the pump. During the 8-day run buffer fluid losses were higher than would normally be expected. When liquid level dropped below the sight glass monitoring range the run was terminated and the pump shut down to protect against possible mechanical damage.

   While this occurrence cut the planned calibration run short by one or two days, it did not materially compromise the data obtained. However, it did point out the need for a means of adding buffer fluid while the pump is in service. Such a reservoir will be added before the next run (see later discussion for further developments on this problem).

4. The pressure differential instruments used to monitor pressure drop across the individual exchangers as one means of detecting coke deposition on the inside tube walls were erratic in their performance. The problem was attributed to over sensitivity to pressure variations and possibly aggravated by safety valve leakage. Amplifier boards with a dampening feature to increase the time constant of the instruments were installed and performance appears to be substantially improved.

5. A number of small bleed and bypass valves with Teflon seats and packing developed leaks when they were exposed to hot oil that exceeded the maximum use temperature for the Teflon. They have been replaced by valves with stainless steel seats and asbestos packing.

6. When checking the energy balance on the unit it was determined that heat losses from the electric heaters were about 30% higher than had been anticipated. It was determined that the major loss was through the front face of the heaters which contain a 1" x 9' long quartz view port. Very substantial heat was being radiated to the outer shell of the heater through this viewing cavity in the refractory.

   On the subsequent run, this view port cavity was packed with insulating material and the heat loss to the front of the cabinet was substantially reduced. Heat losses were further reduced by reducing the purge air rate and insulating the external exchanger flanges.

At the conclusion of the hot calibration run the unit was shut down for the required alterations and repair. The three exchanger tubes were removed and disected to determine if any coke had formed on the inside tube wall. Of course, no significance could be assigned to the rate of coke buildup during this run since it had been carried out under frequently changing process conditions and had been at the most severe conditions only a few hours just prior to shutdown. However, some coke was found on the wall of the tubes and it was observed to be generally heavier on exchanger D which had been operated throughout the run at the lowest mass velocity (and, therefore the highest inside film temperature). This was encouraging evidence that the unit was performing as anticipated and that coke laydown did indeed occur with relatively short time exposure to these simulated process conditions.

The unit was now readied for the first planned test run.

3.2.3 Test Run No. 1

It had been known for some time that the Bayway No. 7 Atmospheric Distillation Unit, which provides the crude oil feed to the Coking Test Unit, was going to be shut down for a three to four week planned maintenance turnaround starting on April 1st. This means that no feed would be available and that testing would have to be interrupted during this period. Therefore, it was planned to schedule at least one of the more severe (and probably shorter) planned runs from the test matrix between the completion of the calibration run and the start of the refinery turnaround.

Therefore, Test No. 1, planned for a nominal 60 k Btu/hr ft^2 flux rate and a 650°F crude inlet temperature was initiated on March 21st.

During startup, the safety valves on Heater "C" (300 lbm/ft^2 sec mass velocity) released prematurely and this exchanger had to be shut down. In order to obtain important data at the above mass velocity, it was decided to reduce the mass velocity in Heater "B" from 450 to 300. Heater A was run at its design mass flow rate of 600 lbm/ft^2 sec.

About 42 hours into the run the test had to be abruptly terminated when the leakage rate of the buffer fluid on the booster pump became substantially greater than it had been during the previous calibration run. The refill reservoir had not yet been installed and the leak rate was such that the pump obviously had to be shut down for repair.

The pump supplier, Sundyne, have now inspected the pump and have recommended replacement of the impeller housing which apparently had a manufacturing defect in the casting. The replacement will be provided by Syndyne under warranty. Initial indication is that the parts can be obtained and installed within the three to four week planned refinery downtime. We are waiting confirmation from Sundyne on this schedule.

Meanwhile, the exchanger tube sections from Test No. 1 have been removed and are being examined. Initial inspection indicates that a significant amount of coke was deposited on the wall of Exchanger "D" which was operated at the lowest (150 lbm/ft^2 sec) mass velocity. The coke thickness also appears to show a definite gradation in thickness - increasing toward the exchanger outlet and - indicating the expected dependence on bulk fluid and inside film temperatures.

While these preliminary observations are encouraging, detailed analysis and interpretation of the data will be based on a comparison of what is found in the other exchangers which were run at higher mass velocities (lower film temperatures) during this abbreviated run.

The data and analysis from this and subsequent tests will be reported in later Program Technical Reports.

3.2.4 Planned Work

It is anticipated that testing will be resumed on or about May 1st. A matrix of eight tests is planned which will probably cover a total period of 28 to 30 weeks. Some modifications of the exact test sequence and conditions will probably be appropriate in some of the later tests based on an analysis of earlier test results.

3.3 Fluidized Bed Heat Transfer Studies

3.3.1 Background Information

The objective of the Fluidized Bed Heat Flux Studies is to quantitatively define both the peripheral and the tube-to-tube maldistributions of heat input to tubes immersed in a fluidized bed. The maldistribution patterns will be determined as a function of controllable design parameters including tube size, spacing, orientation and fluidization velocity.

The data to satisfy the requirements of this task are being obtained in two separate series of tests. The principle tests will be carried out in a "hot" fluidized bed facility. These tests will determine the overall level and pattern of heat transfer to tubes in a fluidized bed. Some complementary ambient temperature studies, which are now completed, have defined the conductive/convective component of the heat transfer mechanism. By comparing results from the high temperature and ambient tests the radiation component will be determined by difference.

A detailed discussion of the facility designs and Task Plan for this part of the Program is given in the Quarterly Technical Report No. 3, dated April 25, 1977. The interested reader is referred to that report for additional information.

3.3.2 High Temperature Heat Flux Tests

The Heat Flux Test Unit which will be built for the high temperature tests has been designed and the vendor has been released to begin fabrication. Delivery is promised for early July.

Ancillary support equipment including an air fin cooler and air metering system is on order. Other miscellaneous items required to complete the system are in various stages of procurement. Onsite construction activities are planned to commence during 2nd Quarter 1978.

3.3.3 Ambient Temperature Heat Flux Tests

The conductive/convective heat transfer measurements on single tubes and bundles were completed in conjunction with the Flow Visualization Tests discussed earlier in this report. The results have been reported in previous Program Quarterly Technical Reports. The remaining unreported data obtained during the tests with the reduced tube-to-grid spacing and with alternative bed particle size distributions are reported here under Section 3.1.3.

REFERENCES

1. Cherrington, D. C., Golan, L. P., Hammitt, F. G., "Industrial Application of Fluidized Bed Combustion Single Tube Heat Transfer Studies", Fifth International Conference on Fluidized Bed Combustion, Washington, D.C., December 1977.

2. Saxena, S.C. and Vogel, G.J., "The Measurement of Incipient Fluidization Velocities in a Bed of Coarse Dolomite at Temperature and Pressure", Trans. I. Chem E. Vol. 55, pages 184-189, (1977).

3. Louis, J.F., "Modeling of Fluidized Bed Combustion of Coal", Quarterly Technical Report No. 1, DOE Contract E(49-18)-2295, August 1976, M.I.T. Energy Laboratory, Cambridge, Mass.

4. Cranfield, R.R., and Geldart, D., "Large Particle Fluidization", Chem. Eng. Science, Vol. 29, pages 935-947, (1974).

5. Ergun, S., Chem. Eng. Progress, Vol. 48, page 89 (1952).

6. Wen, C.Y. and Yu, Y.H., "Mechanics of Fluidization", Chemical Engineering Progress Symposium Series, Vol. 62, pages 100-111, (1966).

7. Cherrington, D.C. et al, Industrial Application Fluidized Bed Combustion Quarterly Report No. 6, DOE Contract EX-76-C-01-2471, October-December 31, 1977.

8. Cherrington, D.C. et al, Industrial Application of Fluidized Bed Combustion Quarterly Report No. 5, DOE Contract EX-76-C-01-2471, July-September 1977.

FORM ERDA 535
(2/1/77)

U.S. ENERGY RESEARCH AND DEVELOPMENT ADMINISTRATION

MILESTONE PLAN AND MANAGEMENT REPORT

1. Contract Identification	Industrial Application of Fluidized Bed Combustion - Category III Indirect Fired Heaters
2. Reporting Period	through 3/31/78
3. Contract Number	EX-76-C-01-2471
4. Contractor (name, address)	Exxon Research and Engineering Company P.O. Box 101 Florham Park, New Jersey 07932
5. Contract Start Date	June 30, 1976
6. Contract Completion Date	March 31, 1979

7. Identification Number	8. Reporting Category (e.g., contract line item or work breakdown structure element)
1	Project Management
2	2-Dimensional Flow
3	Process Stream Coking Studies
4	Fluidized Bed Flux Studies
5	Unit Operability Studies
6	Econ. & Applications Eval.
7	Demo. Unit Design
8	Commercial Unit Design
9	Demo. Unit Fab. & S/U
10	Demo. Unit Operation

9. Fiscal Years and Months

T.Q.'77 | FY '77 | FY '78 | FY '79

J A S O N D J F M A M J J A S O N D J F M A M J J A S O N D J F M A M J J A S O N D

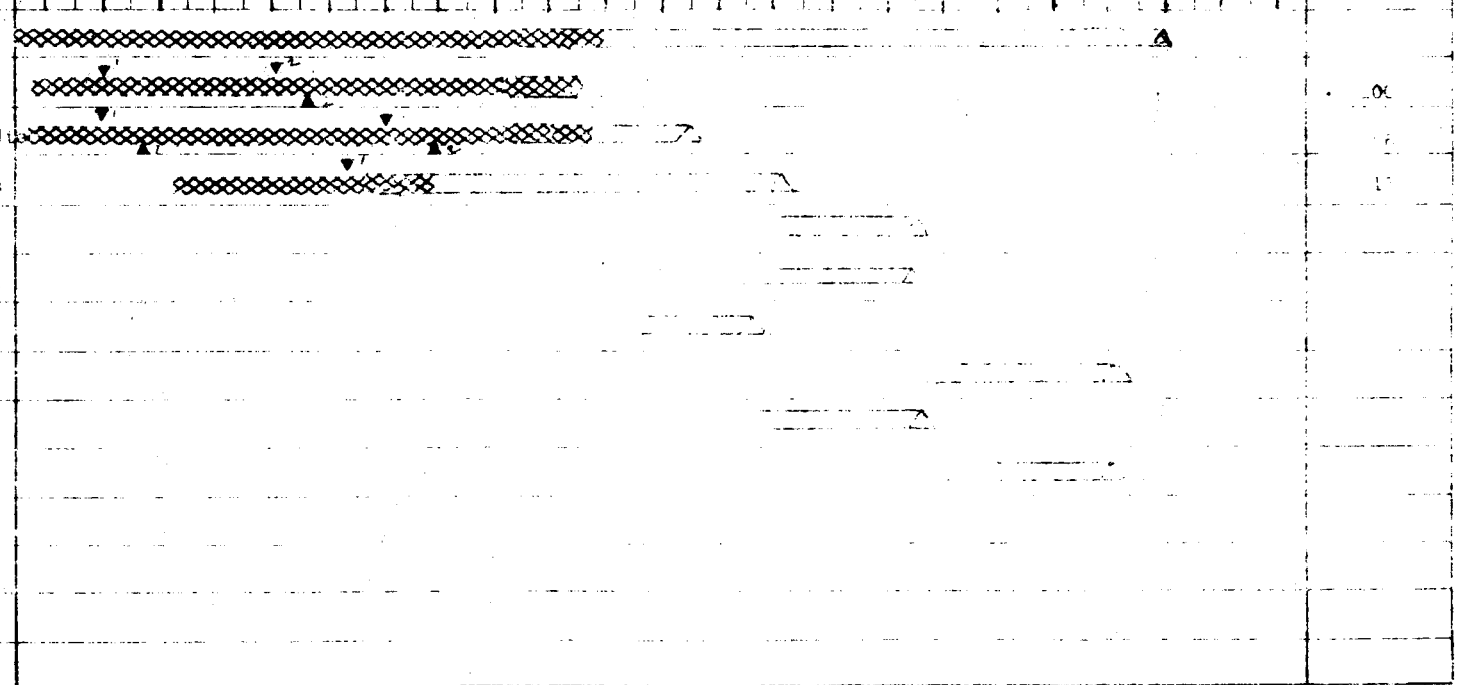

10. Percent Complete

11. Remarks: 1. ERDA 90% design review
2. Construction complete
3. Testing complete

12. Signature of Contractor's Project Manager and Date

D. C. Cherrington 4/17/78

13. Signature of Operations Officer and Date

FIGURE 1

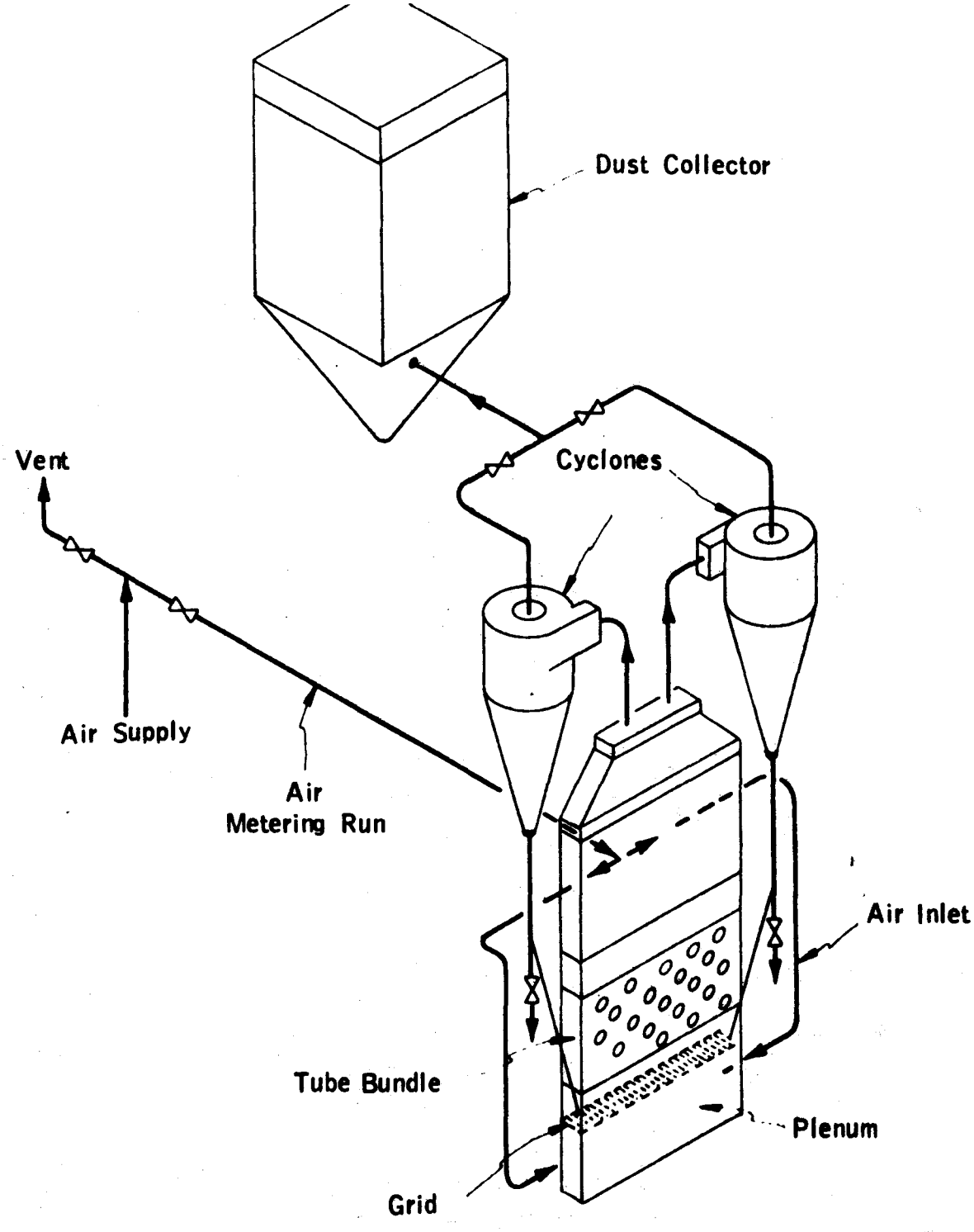

Figure 2

SCHEMATIC-TWO DIMENSIONAL FLOW VISUALIZATION UNIT

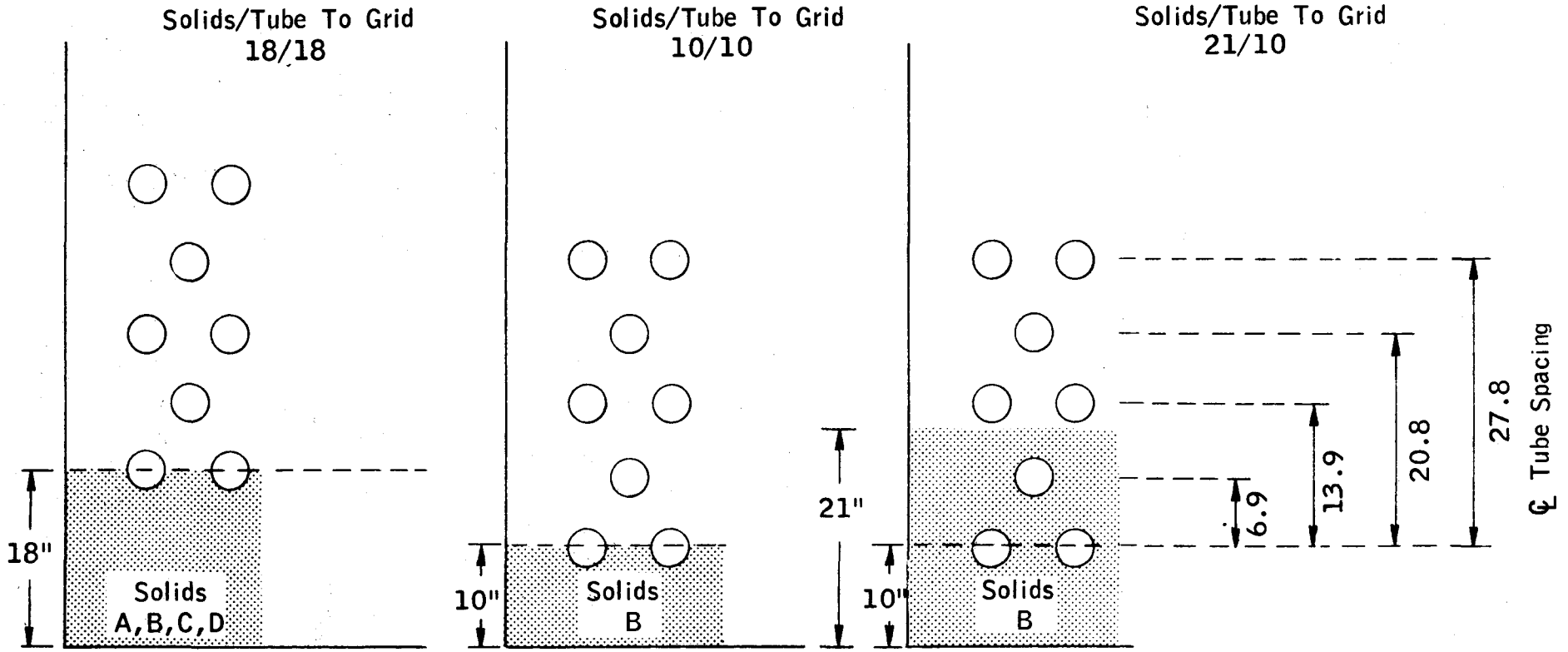

Figure 3

4"-2DE TUBE BUNDLE
TUBE BUNDLE POSITION AND SOLIDS LOADING

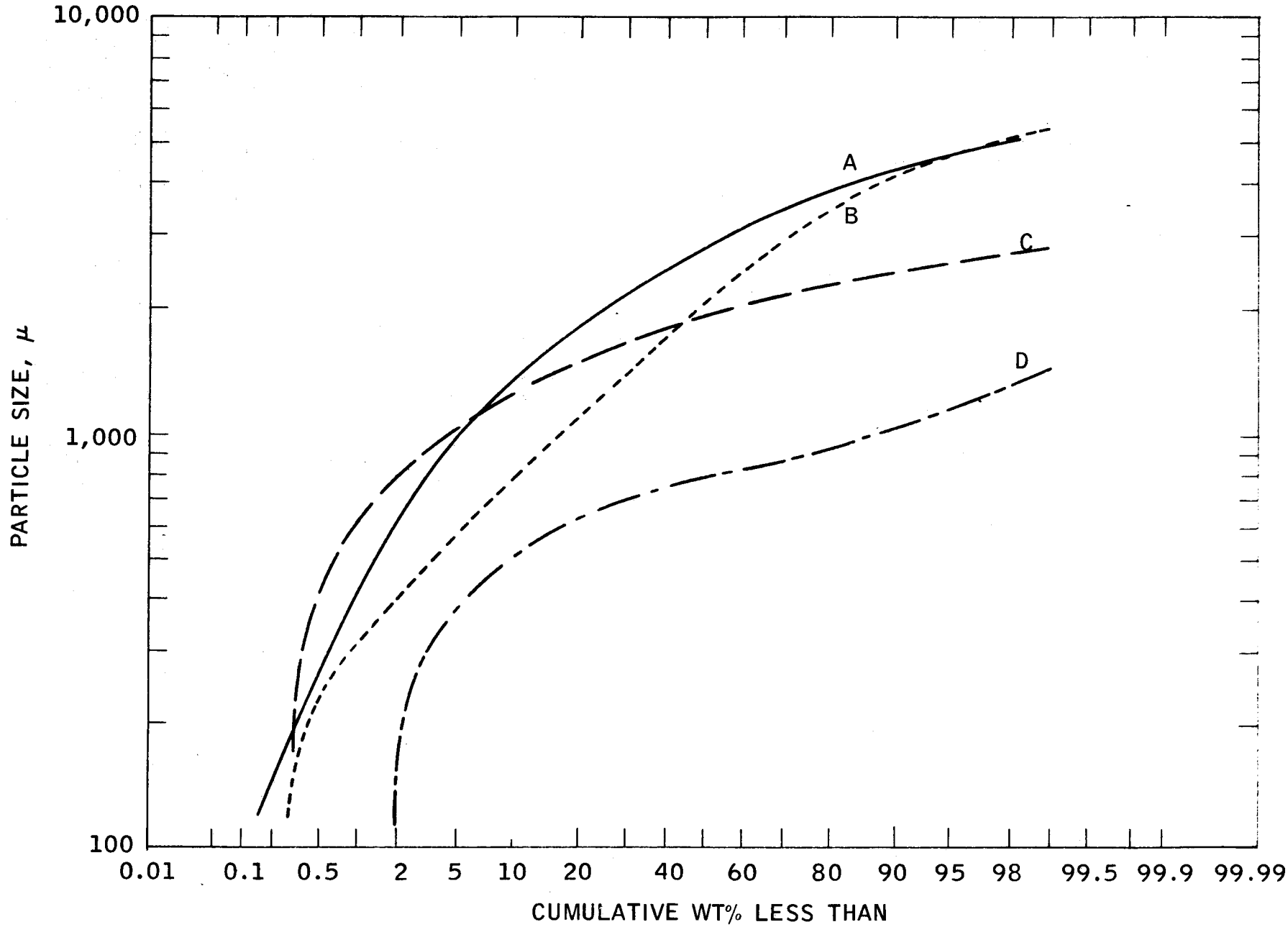

Figure 4

LIMESTONE BLENDS TESTED

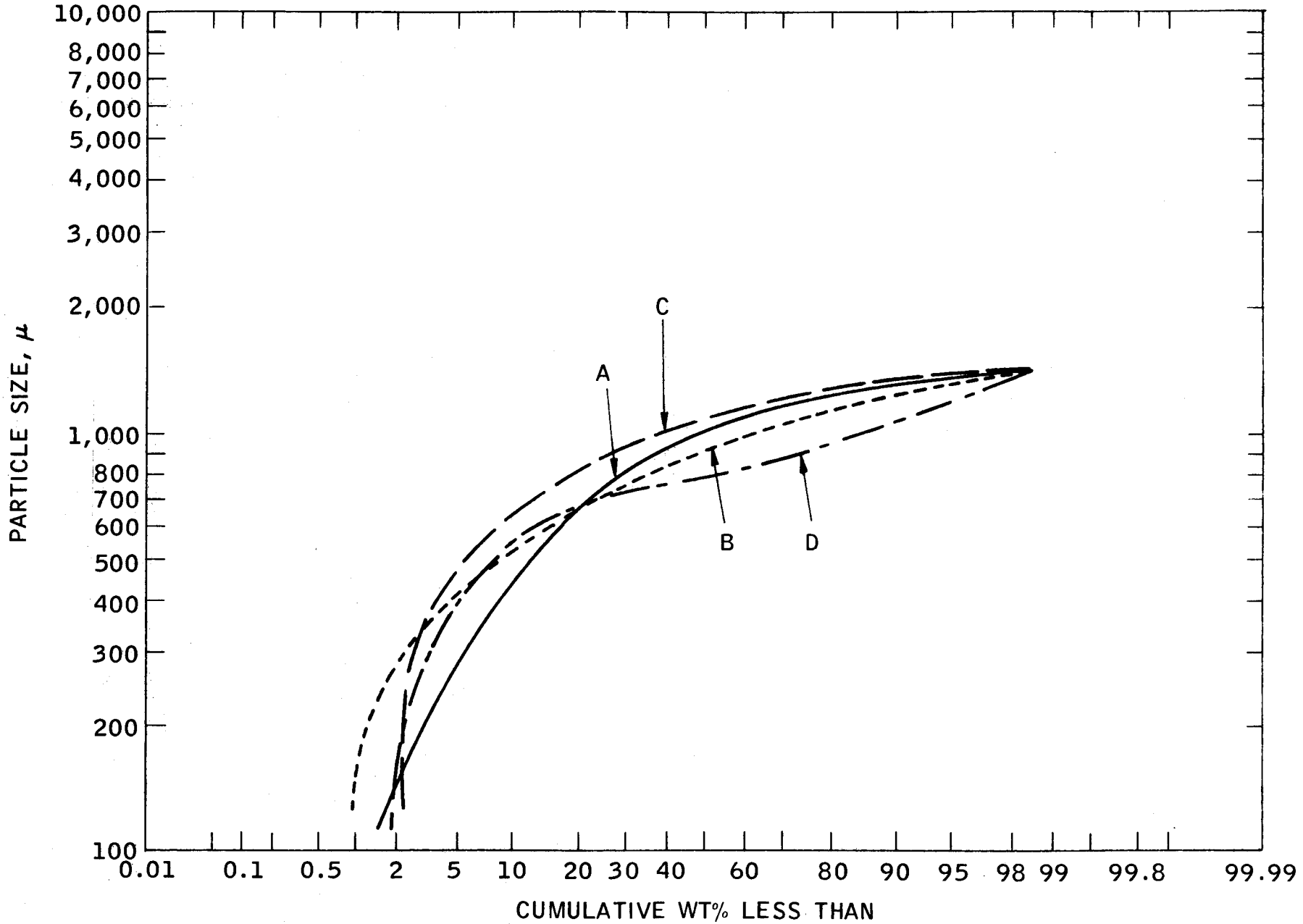

Figure 5

1410 μ MINUS FINES CONCENTRATION IN LIMESTONE BLENDS A, B, C, D

OBSERVED/PREDICTED MINIMUM FLUIDIZATION VELOCITIES

Limestone Particle Blend[1]	Wt. ave. Particle size, μ	Volume ave. Particle size, μ	Experimental u_{mf}, FPS	Predicted u_{mf} Wt. Ave.	Predicted u_{mf} Vol. Ave.
A	2700	1130	2.3	5.9	2.8
B	2000	910	2.2	4.8	2.3
C	1950	1270	2.1	4.6	2.9
D	800	540	1.5	2.0	1.3

1. See Figure 2 for a complete screening of the four limestone particle blends

FIGURE 6

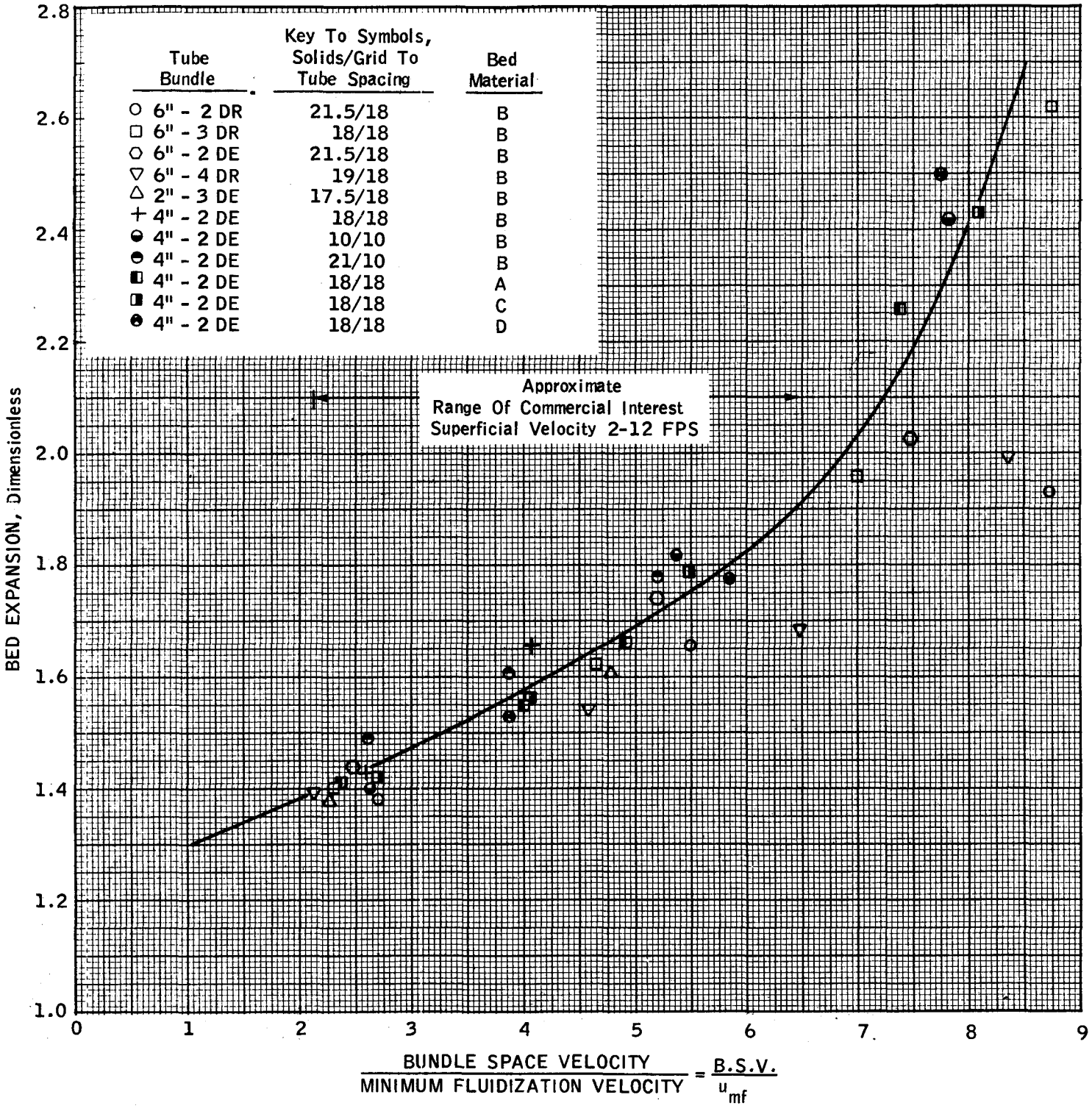

Figure 7

BED EXPANSION CORRELATION

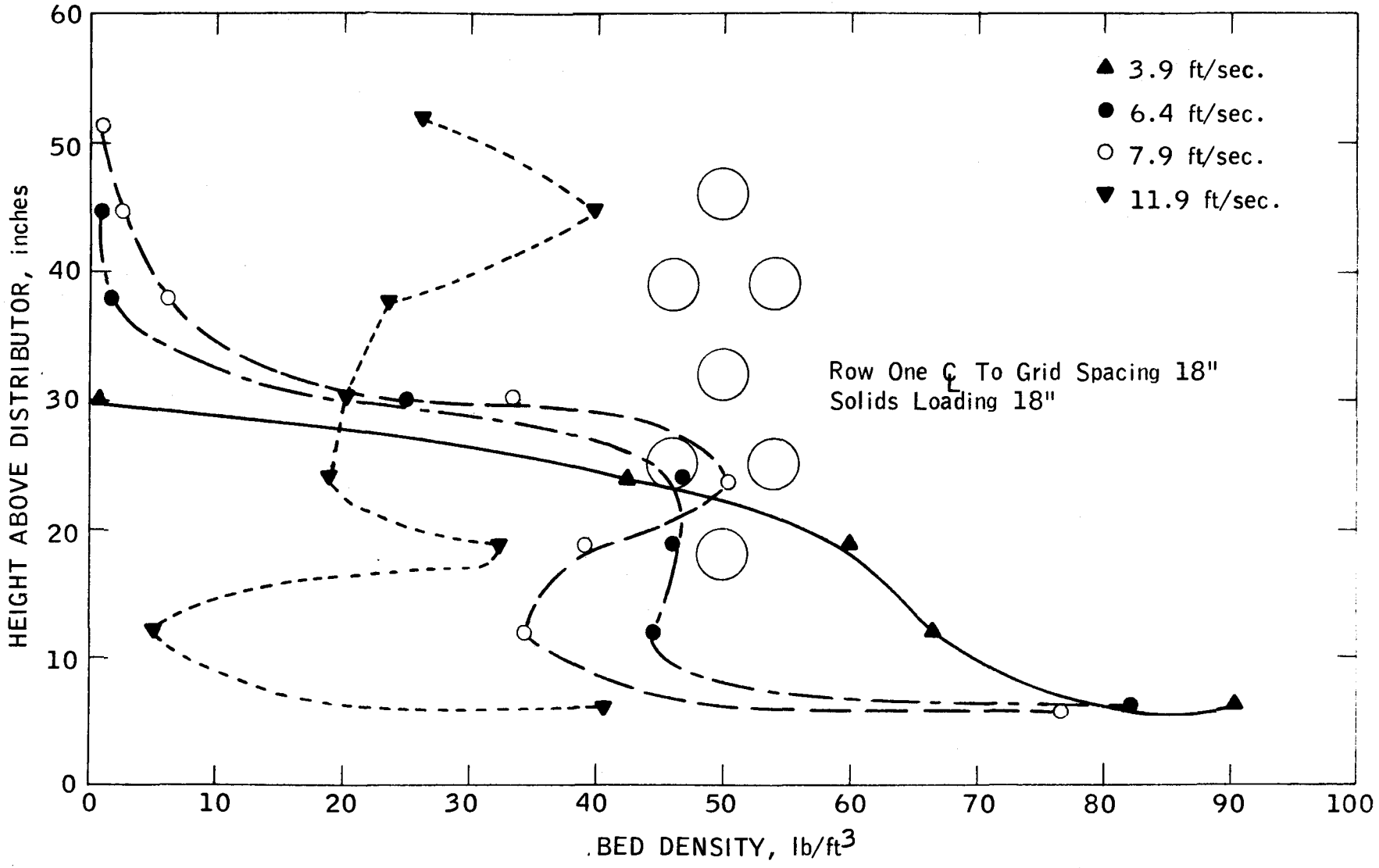

Figure 8a

BED DENSITY PROFILE
4"-2D EQUILATERAL SPACING, PARTICLE BLEND A

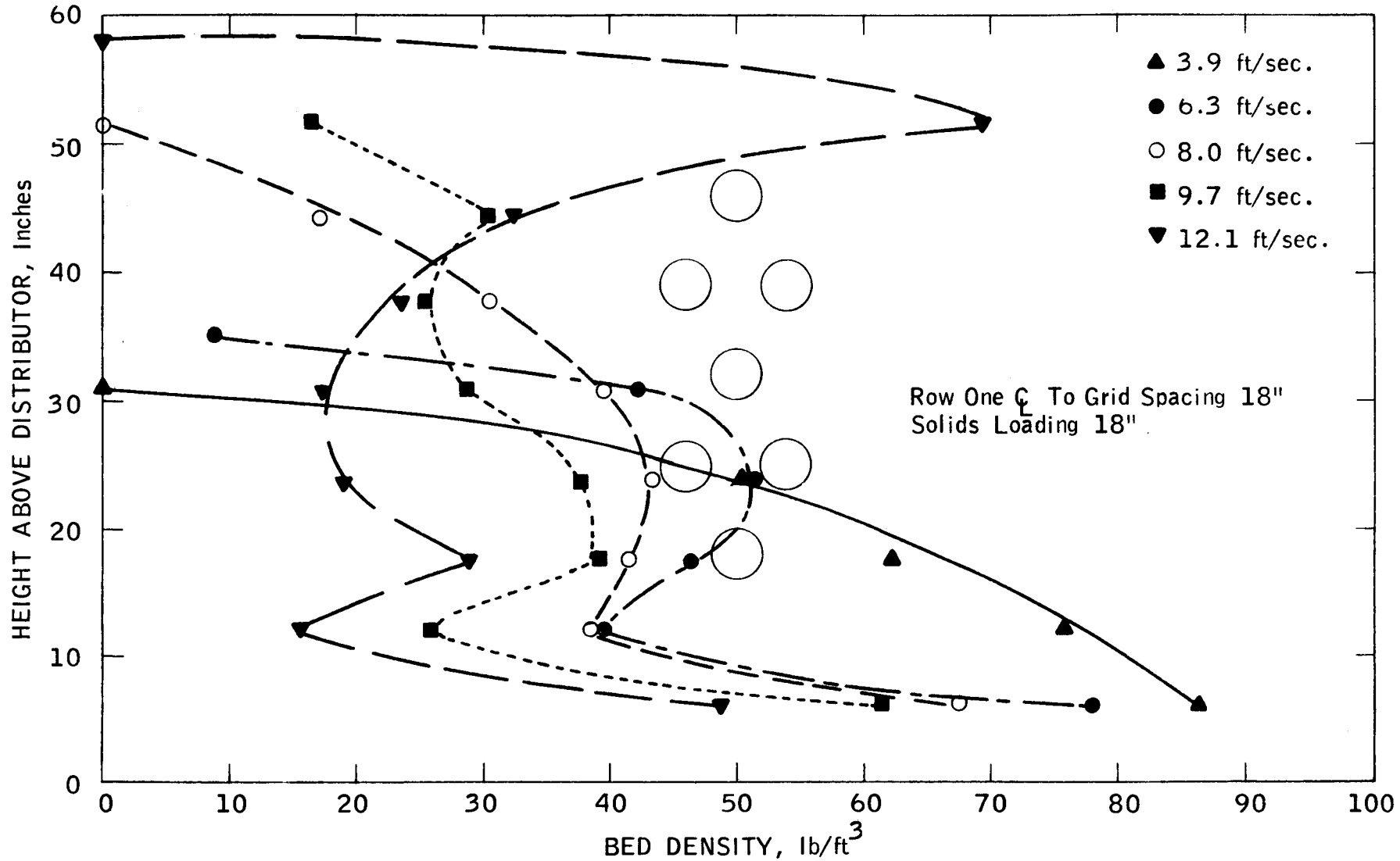

Figure 8b

BED DENSITY PROFILE
4"-2D EQUILATERAL SPACING, PARTICLE BLEND B

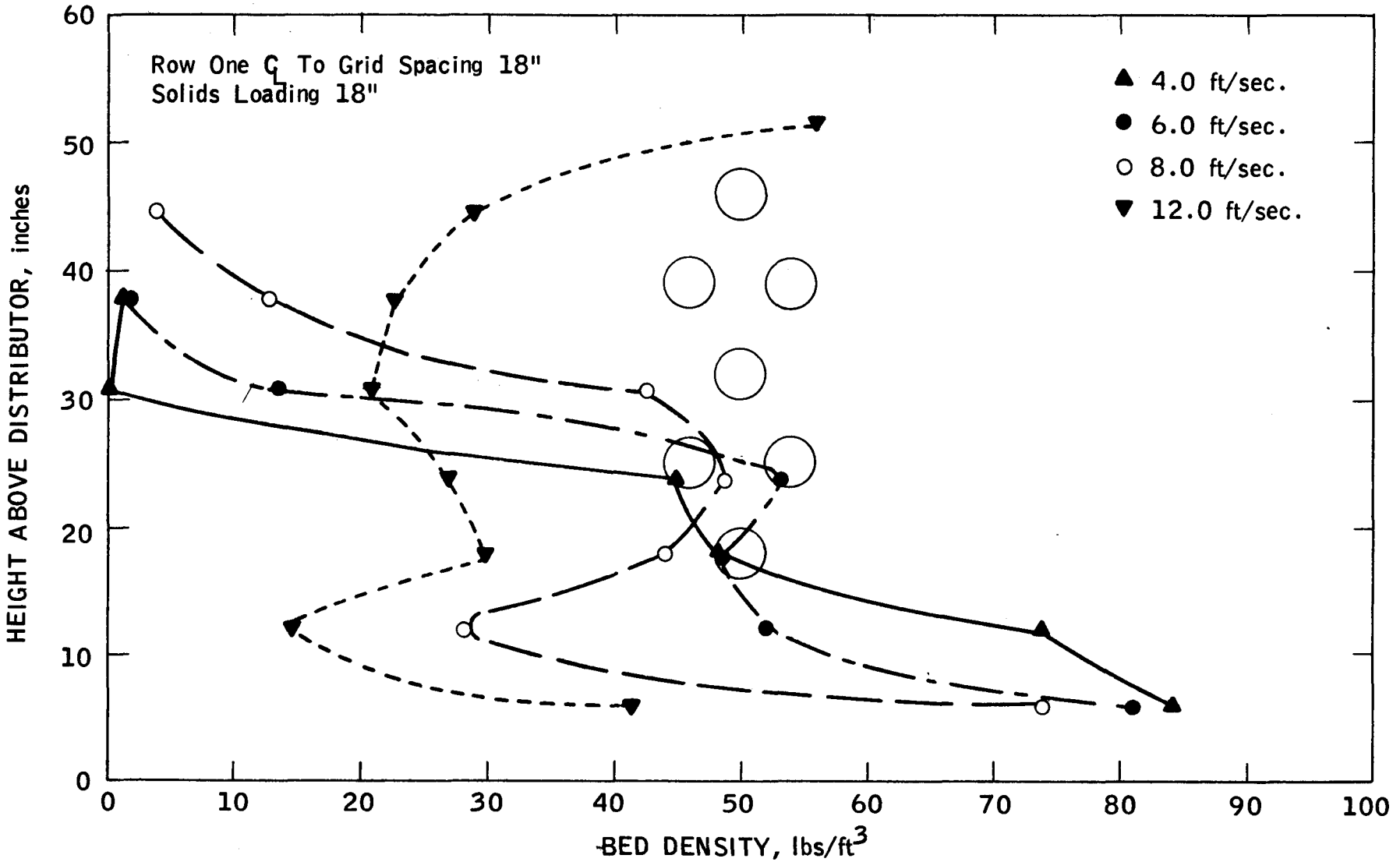

Figure 8c

BED DENSITY PROFILE
4"-2D EQUILATERAL SPACING, PARTICLE BLEND C

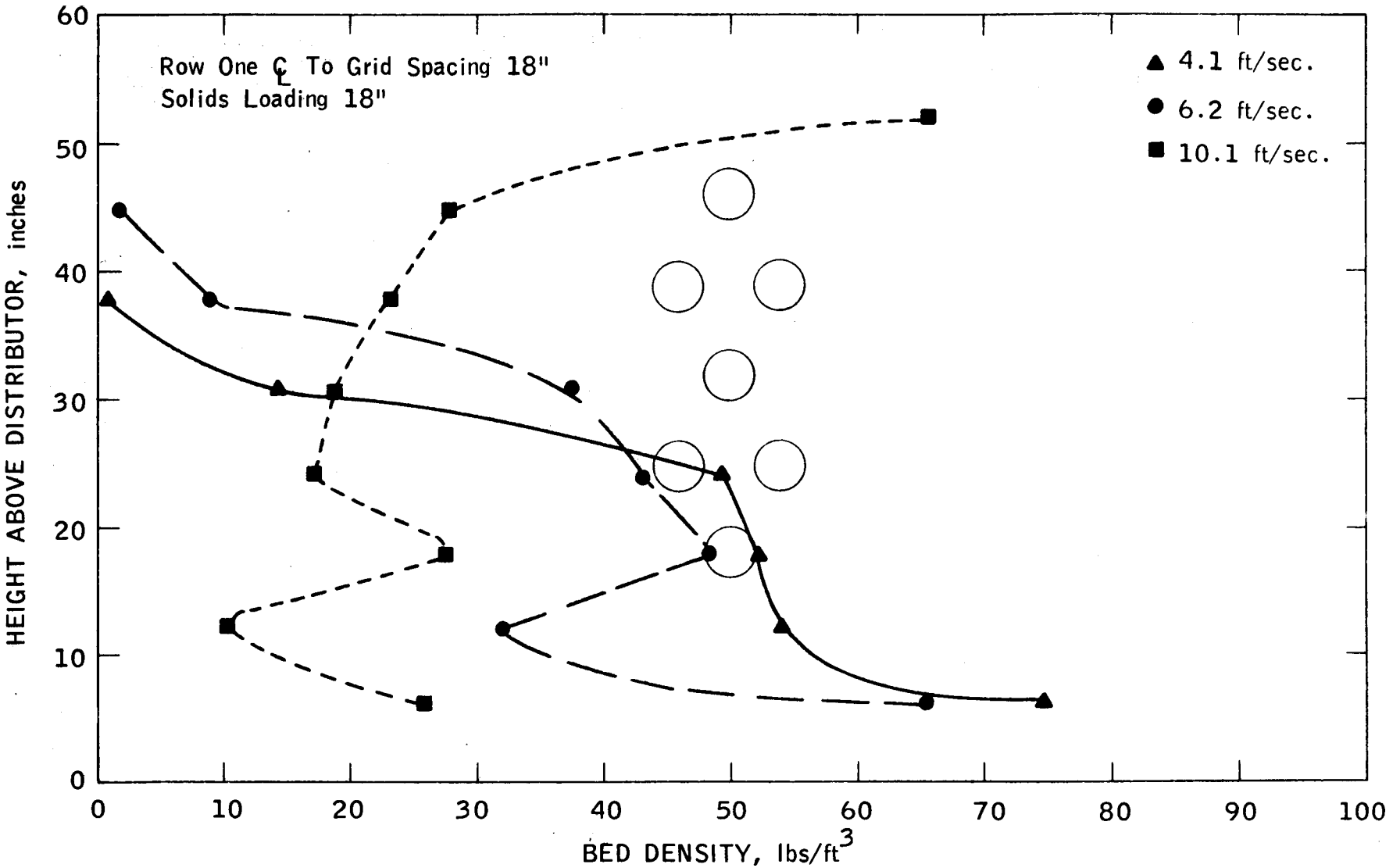

Figure 8d

BED DENSITY PROFILE
4"-2D EQUILATERAL SPACING, PARTICLE BLEND D

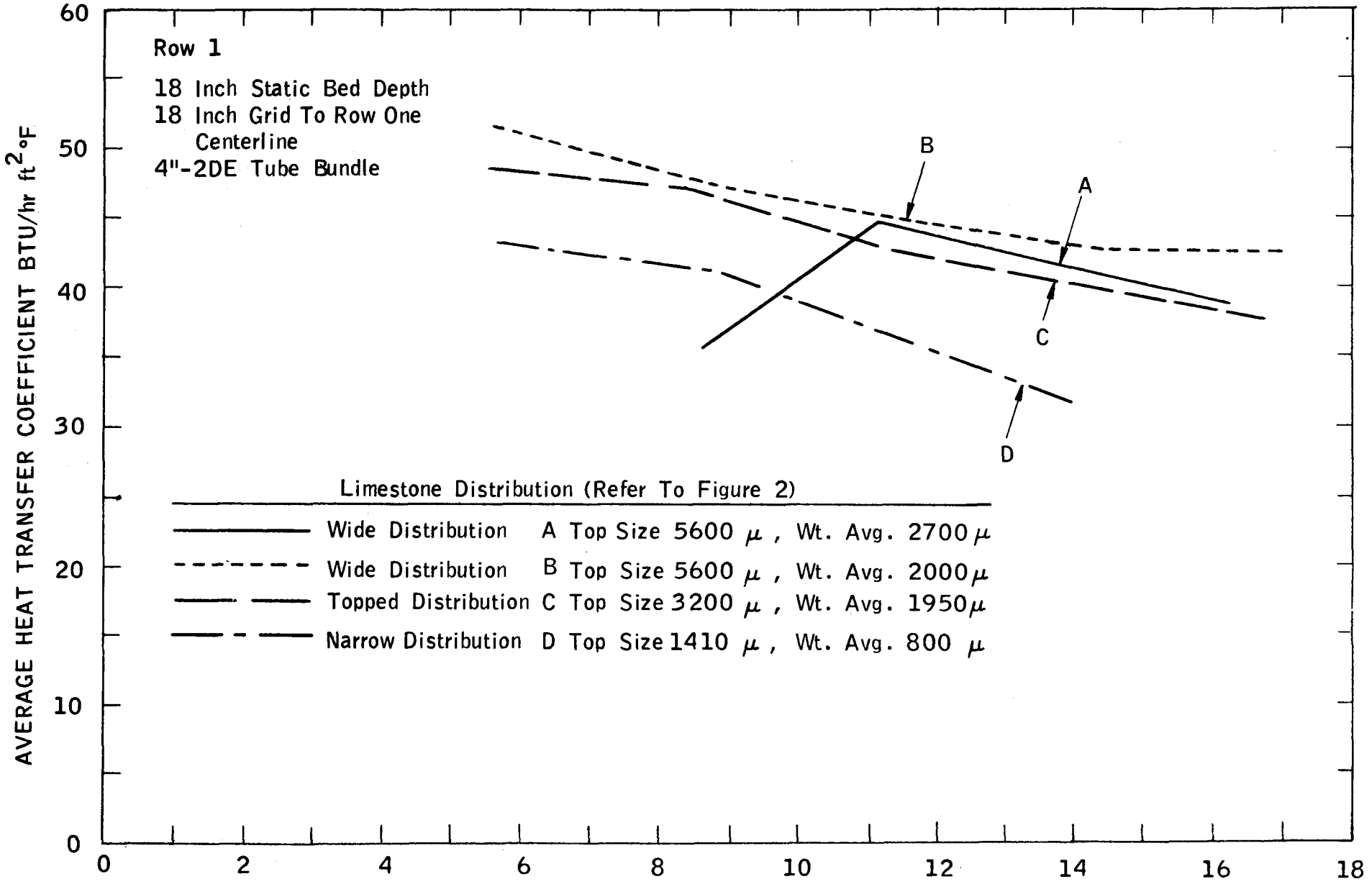

Figure 9

PARTICLE SIZE EFFECT ON ROW 1 HEAT TRANSFER COEFFICIENT

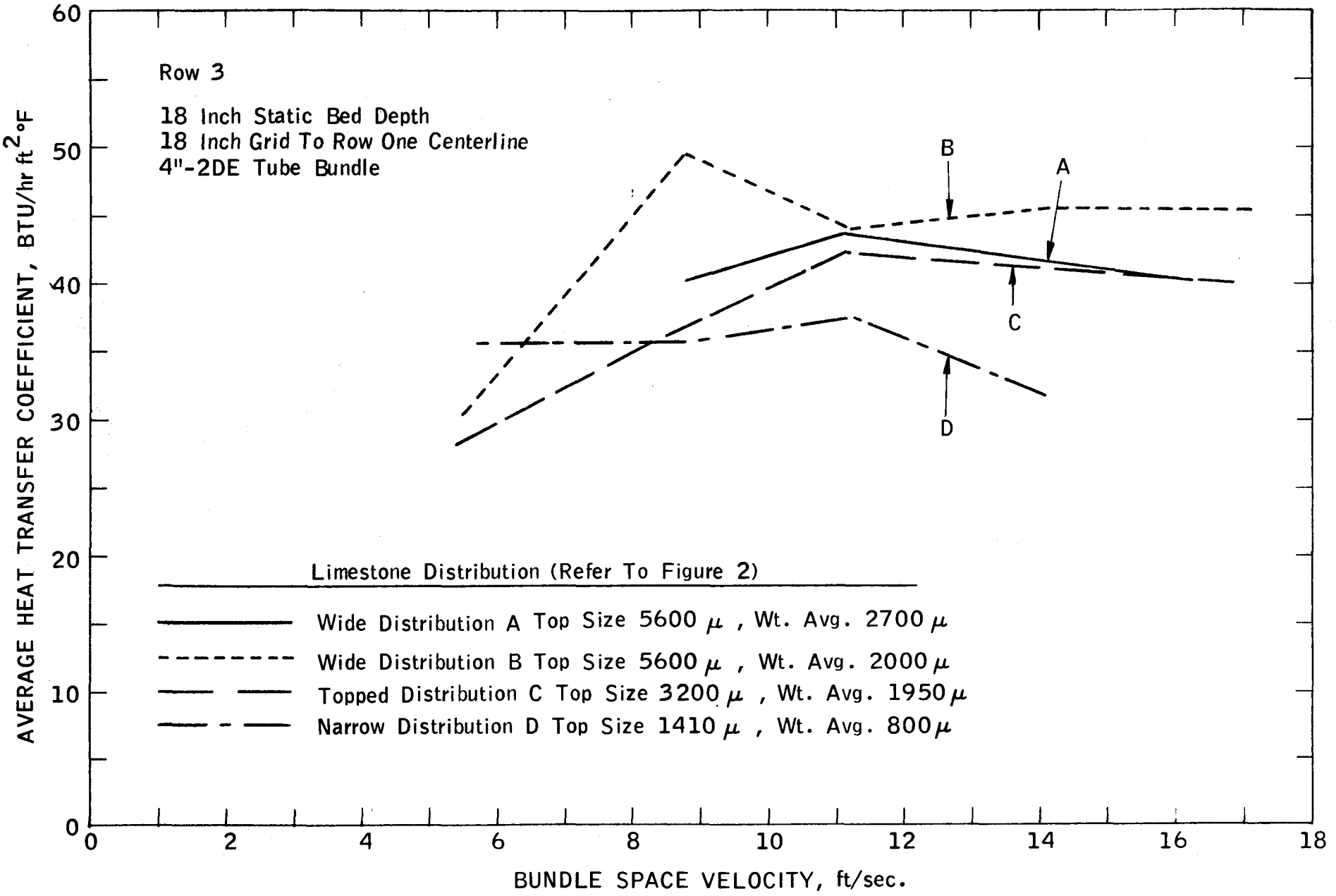

Figure 10

PARTICLE SIZE EFFECT ON ROW 3 HEAT TRANSFER COEFFICIENT

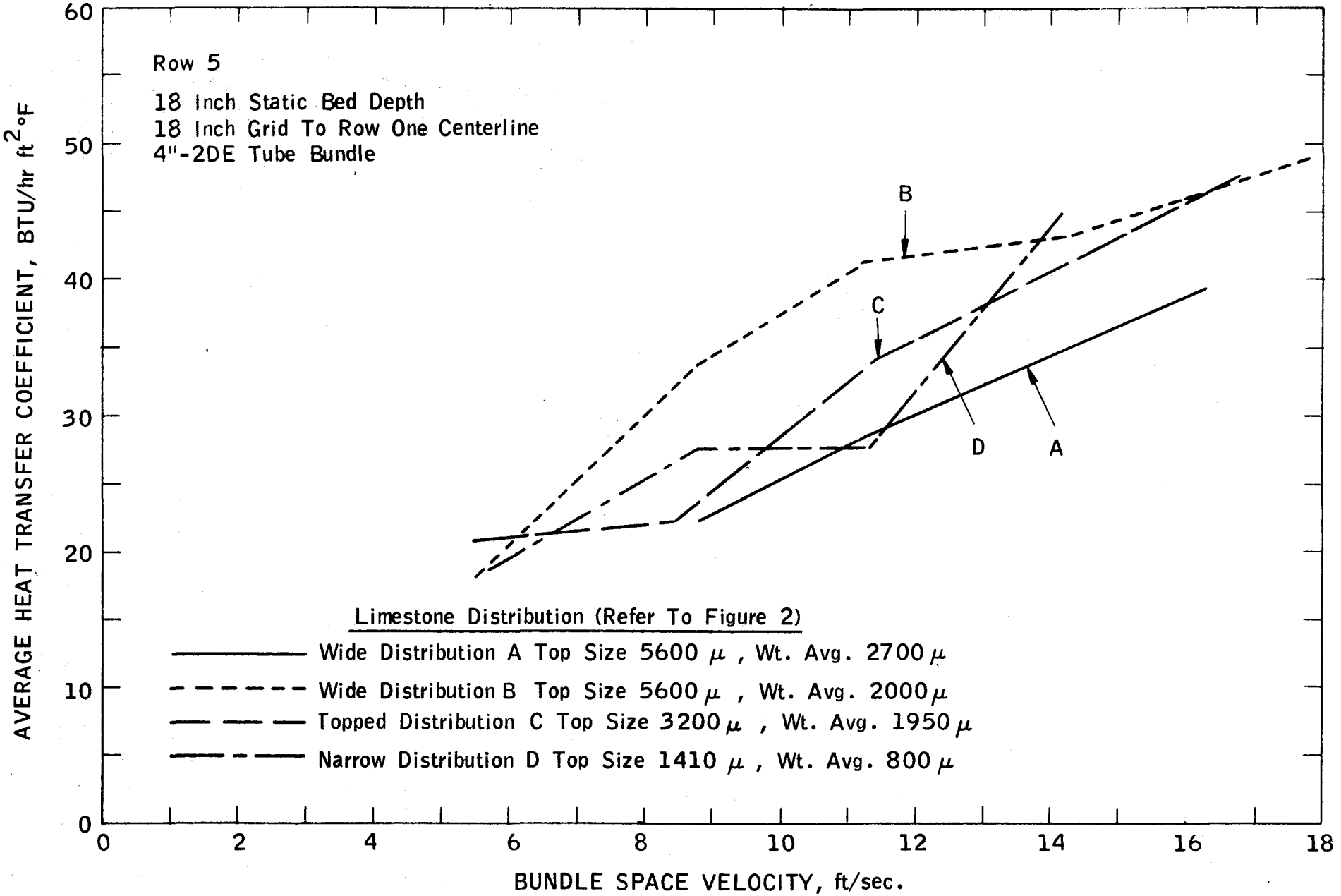

Figure 11

PARTICLE SIZE EFFECT ON ROW 5 HEAT TRANSFER COEFFICIENT

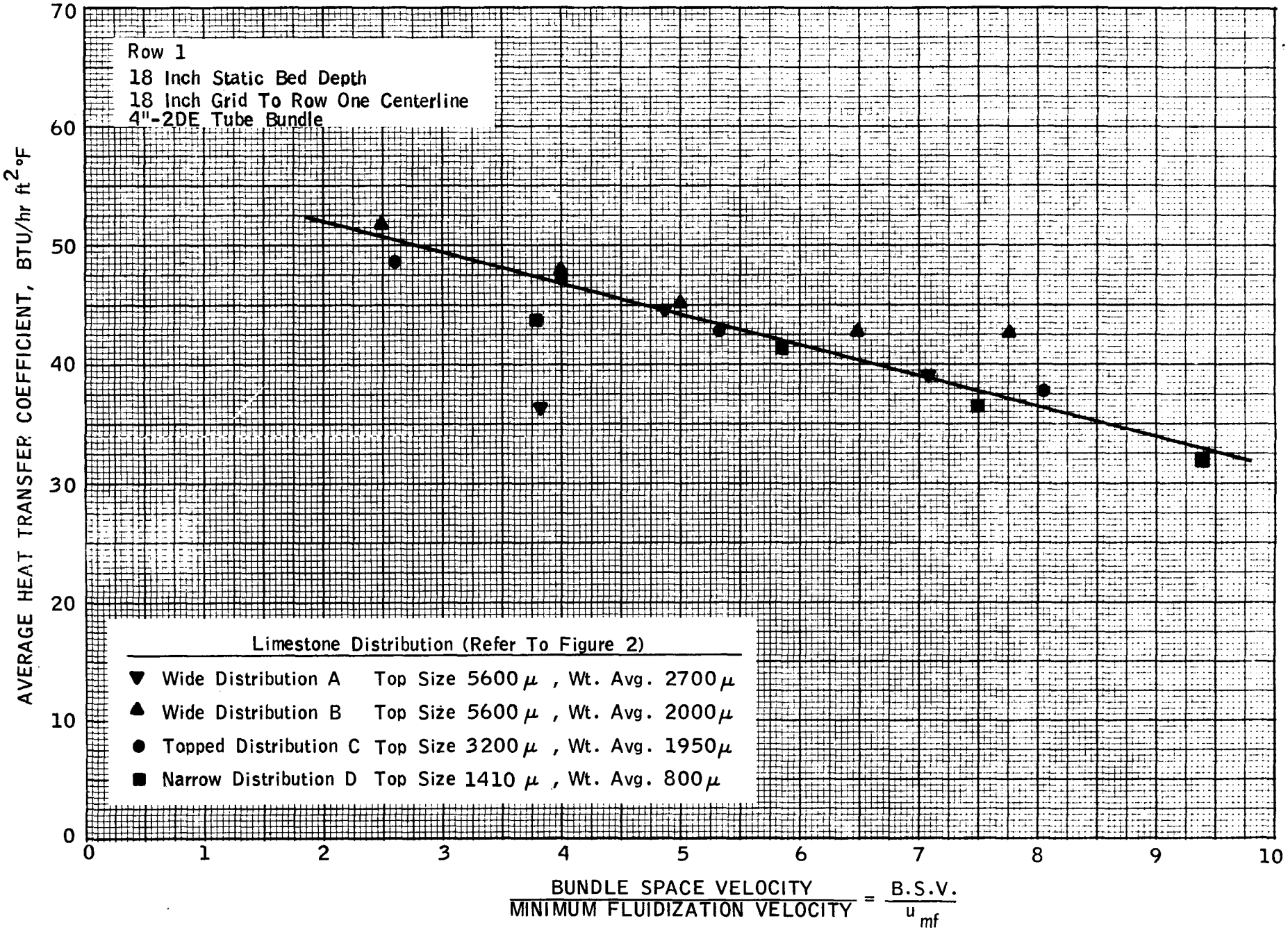

Figure 12

NORMALIZED ROW 1 HEAT TRANSFER COEFFICIENTS

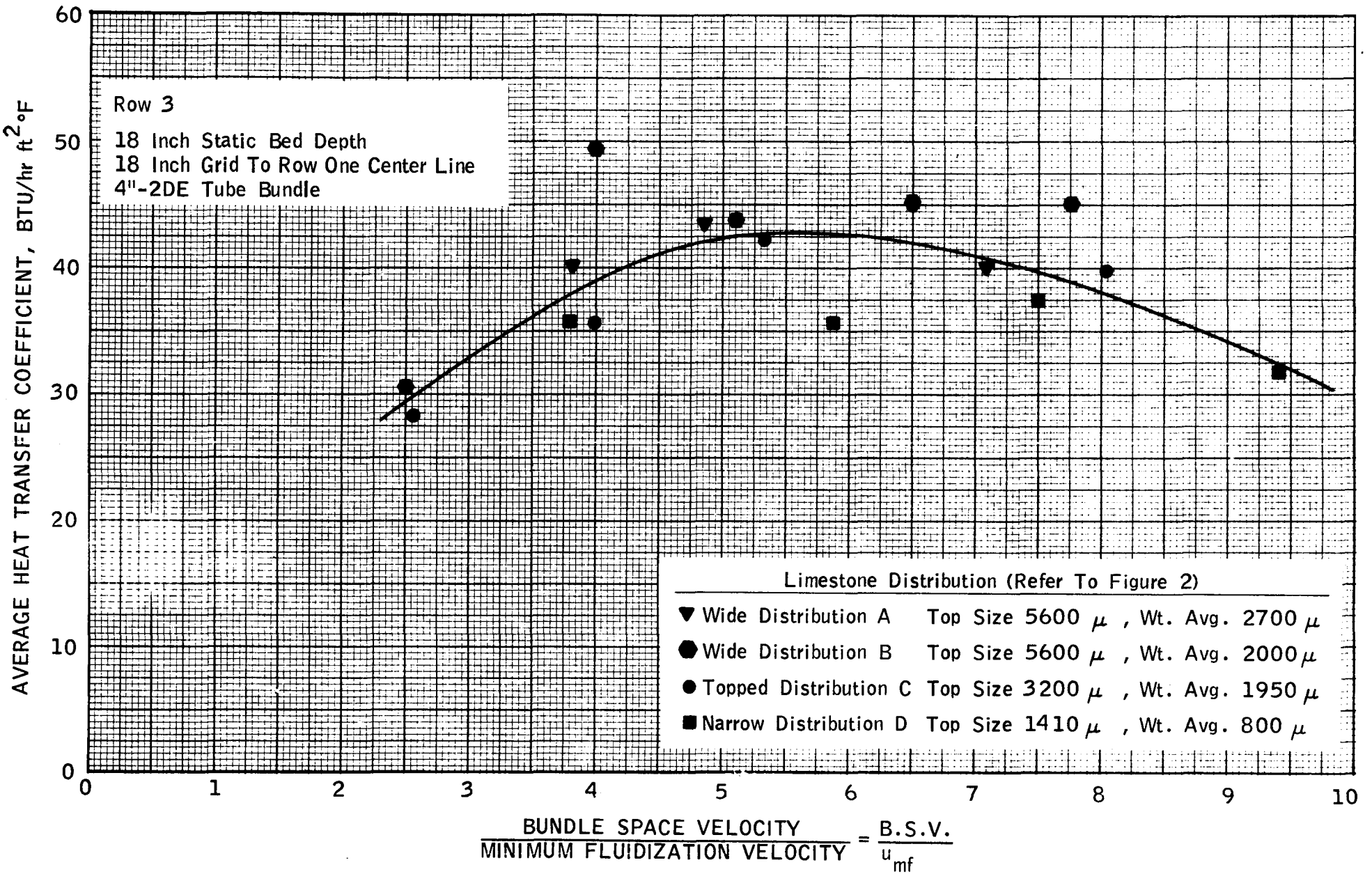

Figure 13

NORMALIZED ROW 3 HEAT TRANSFER COEFFICIENTS

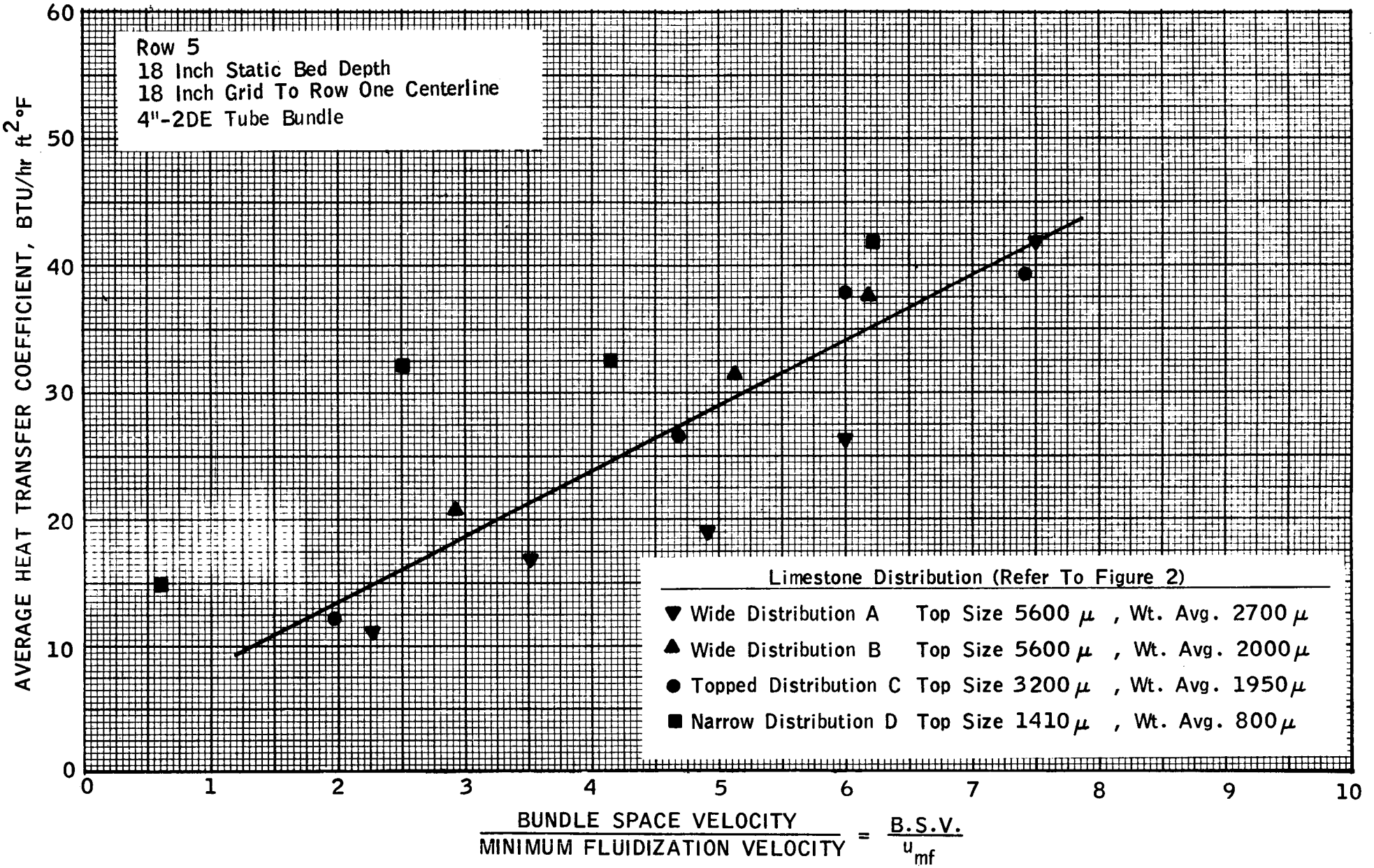

Figure 14

NORMALIZED ROW 5 HEAT TRANSFER COEFFICIENTS

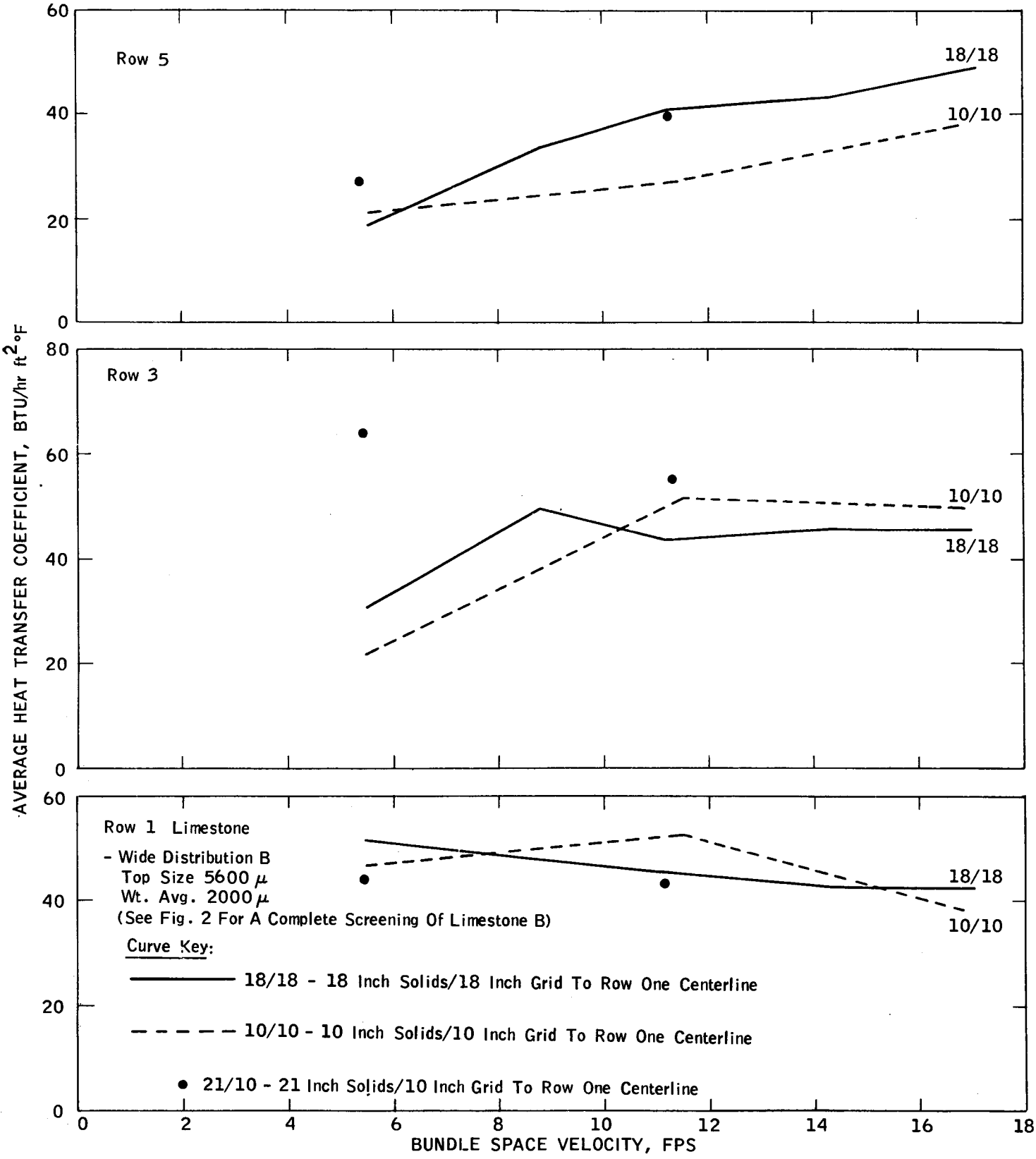

Figure 15

EFFECT OF TUBE TO GRID SPACING ON HEAT TRANSFER COEFFICIENTS
4"-2DE TUBE BUNDLE

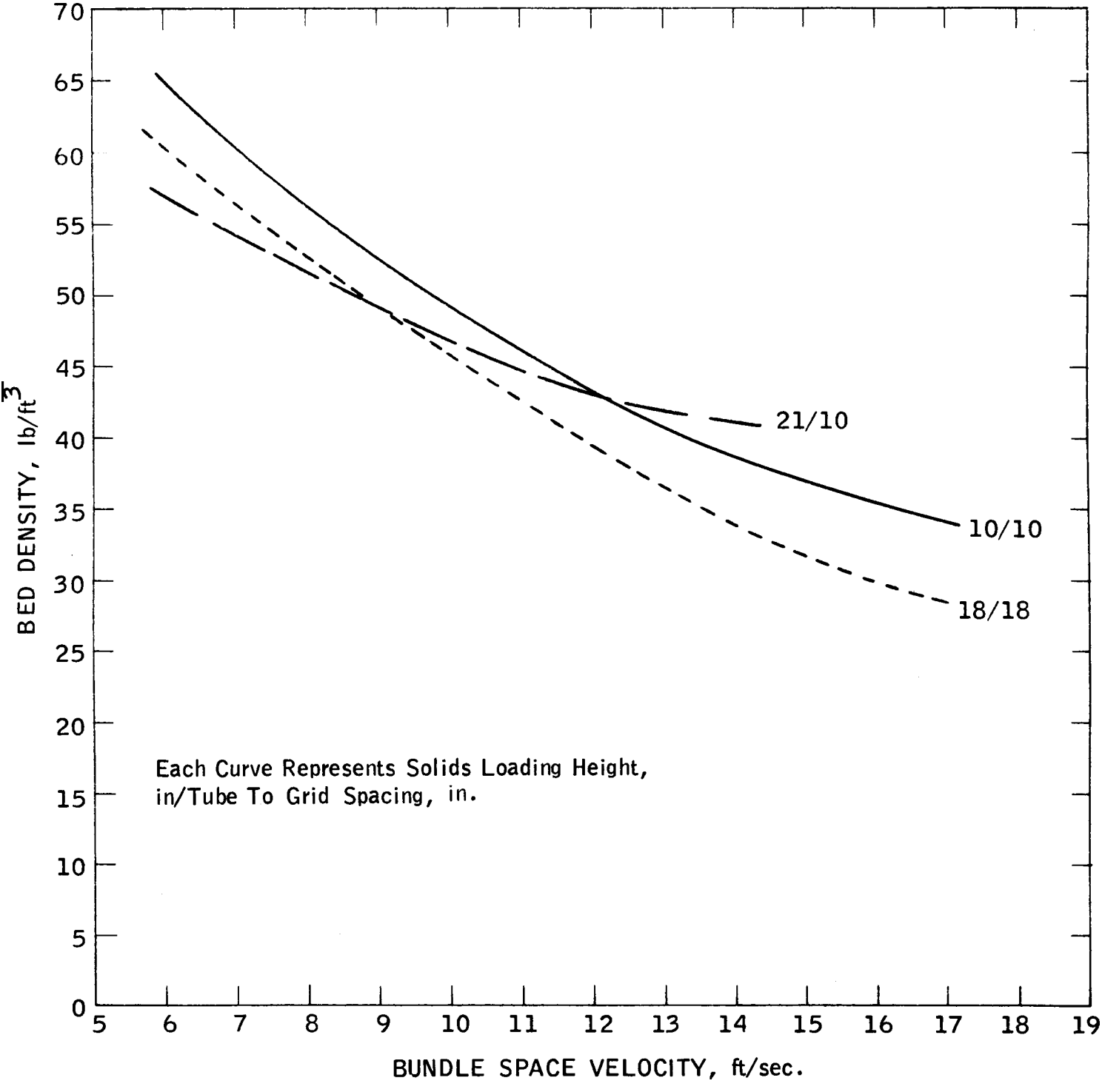

Figure 16

ROW 1 AVERAGE BED DENSITY
4"-2D EQUILATERAL SPACING, PARTICLE BLEND B

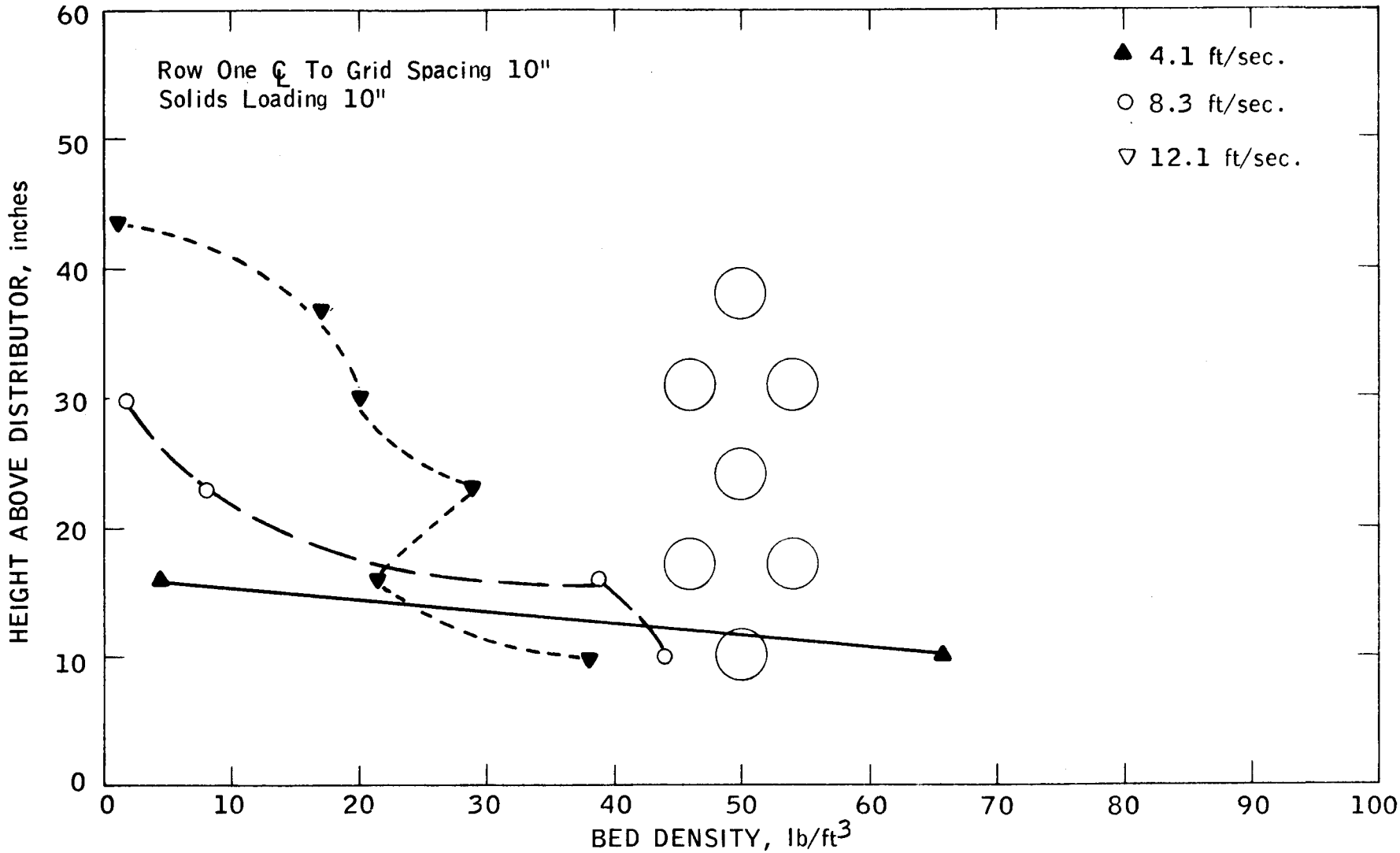

Figure 17a

BED DENSITY PROFILE
4"-2D EQUILATERAL SPACING, PARTICLE BLEND B

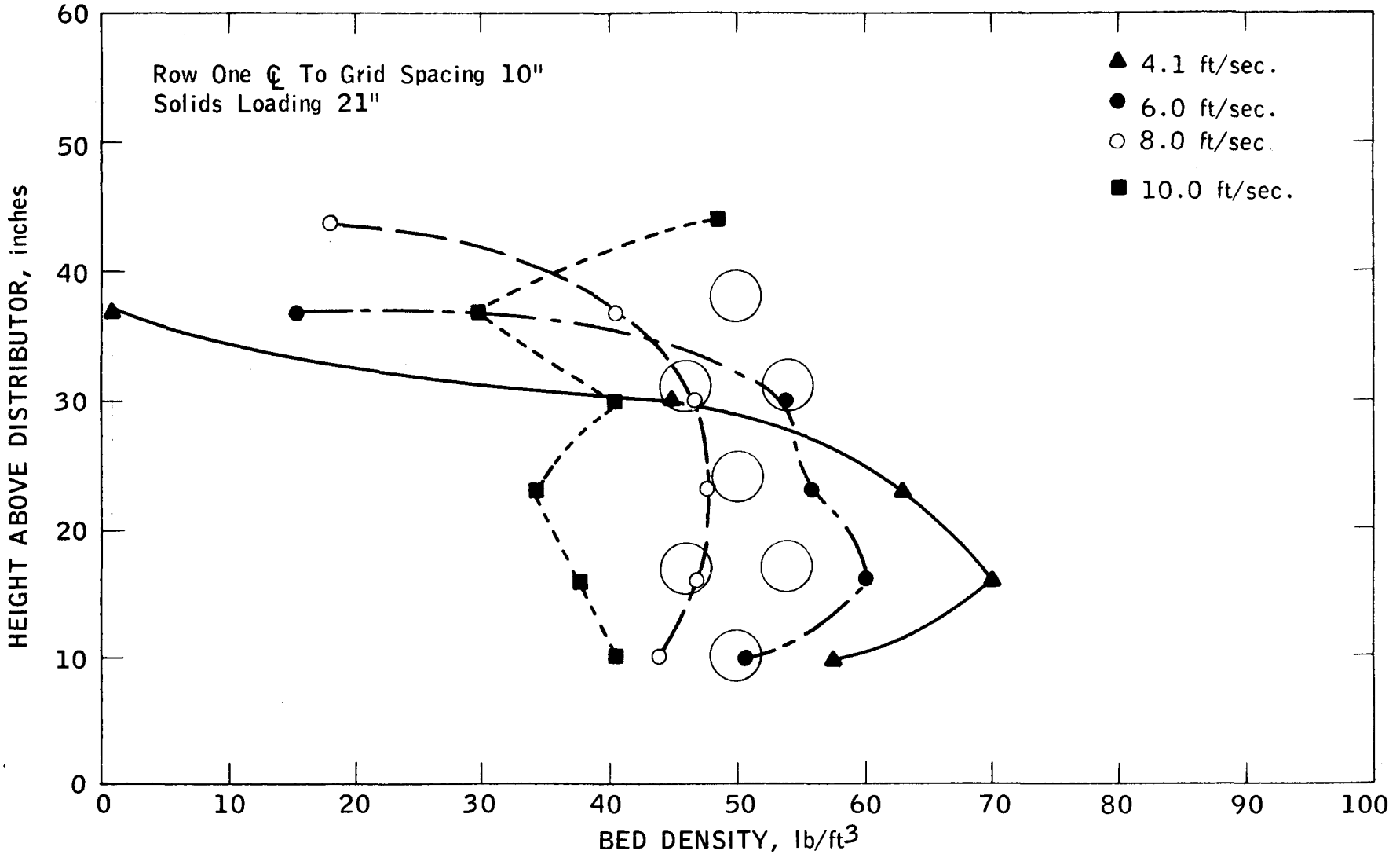

Figure 17b

BED DENSITY PROFILE
4"-2D EQUILATERAL SPACING, PARTICLE BLEND B

APPENDIX I

Reduced Heat Transfer Data

REDUCED HEAT TRANSFER DATA

Bundle Geometry - 4"-2DE
18"- bed solids loading 18"- grid to tube ℄ spacing
limestone material - Blend A

Probe Row No.	Angular Position	Heat Transfer Coefficient (Btu/hr ft^2 °F) Superficial Velocity, FPS 6.2	7.9	11.5
	0/360	15.2	15.9	23.5
	15	17.8	19.2	28.6
	30	22.1	26.5	35.4
	45/315	26.3	31.8	46.1
	60	25.6	30.9	46.3
	75	29.3	38.1	48.0
5	90/270	27.8	35.5	45.5
	105	20.9	32.0	41.3
	120	20.7	28.0	37.4
	135/225	20.7	26.8	36.3
	150	20.9	26.9	38.5
	165	20.5	27.3	40.7
	180	20.2	28.0	42.5
	Average	22.2	28.2	39.2
	0/360	22.9	23.3	22.1
	15	28.3	28.8	27.4
	30	35.5	41.8	34.3
	45/315	(56.6)	62.1	47.8
	60	60.1	63.0	47.1
	75	53.8	58.0	48.5
3	90/270	47.2	44.3	43.5
	105	37.0	41.9	40.4
	120	32.9	39.3	39.9
	135/225	31.9	37.2	38.1
	150	34.4	39.8	40.7
	165	39.7	43.3	45.5
	180	41.4	43.4	45.5
	Average	40.1	43.6	40.0
	0/360	42.0	42.1	24.0
	15	48.4	43.8	26.9
	30	51.8	55.3	34.1
	45/315	50.7	62.0	47.4
	60	45.9	58.9	49.2
	75	37.8	52.2	47.5
	90/270	33.6	46.5	46.1
1	105	28.9	40.2	42.2
	120	27.7	39.4	40.6
	135/225	28.1	37.9	39.2
	150	25.3	34.6	37.1
	165	25.4	33.6	35.8
	180	25.7	34.2	35.7
	Average	36.3	44.7	38.9

( ) Data Pts differ by more than 20%

REDUCED HEAT TRANSFER DATA

Bundle Geometry - 4"-2DE
18"-bed solids loading 18"-grid to tube ℄ spacing
limestone material - Blend B

Probe Row No.	Angular Position	Heat Transfer Coefficient (Btu/hr ft^2 °F) Superficial Velocity, FPS 3.9	6.2	7.9	10.1	12.0
	0/360	12.4	17.3	15.6	23.4	48.7
	15	14.1	26.4	24.1	25.8	57.0
	30	15.3	71.6	33.9	35.2	56.6
	45/315	17.5	73.7	46.3	53.1	59.0
	60	18.7	45.7	52.8	56.4	60.4
5	75	21.6	30.4	39.9	55.8	59.3
	90/270	22.8	30.0	41.7	46.7	51.1
	105	15.7	25.0	32.6	42.3	43.7
	120	16.7	23.1	28.4	37.0	34.1
	135/225	17.6	22.6	30.4	36.0	34.1
	150	19.8	22.7	41.1	44.9	40.5
	165	21.8	24.3	48.5	52.7	42.8
	180	21.0	25.8	50.3	51.1	48.0
	Average	18.1	33.7	41.0	43.1	48.9
	0/360	19.9	28.1	24.7	29.4	28.7
	15	26.6	44.4	30.1	33.2	39.5
	30	32.3	58.1	45.2	45.2	65.6
	45/315	39.3	86.3	69.3	52.4	58.0
	60	43.0	79.4	61.5	48.8	58.6
	75	36.6	58.0	56.2	53.6	46.4
3	90/270	34.3	42.0	43.7	50.0	45.5
	105	27.5	41.1	36.6	44.5	36.4
	120	23.8	39.2	34.4	39.6	35.5
	135/225	24.3	36.5	35.5	39.6	38.7
	150	25.5	39.5	40.4	49.1	41.2
	165	30.5	44.4	46.0	53.0	45.1
	180	30.1	45.6	44.0	51.0	47.4
	Average	30.3	49.4	43.7	45.3	45.1
	0/360	67.1	61.4	44.3	25.0	23.8
	15	70.7	60.2	42.3	30.9	37.5
	30	72.8	71.4	48.4	34.8	60.0
	45/315	77.5	79.0	(61.7)	48.4	58.0
	60	71.6	71.7	62.0	49.5	56.4
	75	56.6	58.9	56.7	58.7	48.5
1	90/270	46.0	44.0	44.1	49.8	45.5
	105	39.3	41.7	43.5	46.7	43.6
	120	36.8	39.2	41.0	44.9	42.4
	135/225	35.1	37.3	37.3	42.4	38.7
	150	33.0	38.4	35.1	42.1	34.3
	165	32.8	37.7	36.0	43.4	33.3
	180	32.3	36.7	34.1	40.5	31.5
	Average	51.7	47.4	45.1	42.8	42.6

( ) Data Pts differ by more than 20%

REDUCED HEAT TRANSFER DATA

Bundle Geometry - 4"-2DE
18"- bed solids loading 18"- grid to tube ℄ spacing
limestone material - Blend C

Probe Row No.	Angular Position	Heat Transfer Coefficient (Btu/hr ft^2 °F) Superficial Velocity, FPS 3.8	5.9	7.9	11.9
	0/360	17.1	(17.5)	18.6	37.8
	15	17.2	17.3	18.4	
	30	18.9	20.2	24.4	
	45/315	19.5	23.2	(44.4)	54.5
	60	21.6	26.2	48.1	
	75	22.2	26.5	43.1	
5	90/270	20.2	25.2	40.7	52.9
	105	22.2	20.8	32.4	
	120	20.2	21.3	30.5	
	135/225	20.1	21.6	34.9	42.0
	150	22.9	22.5	29.8	
	165	22.5	22.2	31.5	
	180	24.0	21.4	34.5	52.5
	Average	20.7	22.0	33.2	47.9
	0/360	19.9	19.0	29.5	22.1
	15	81.1	25.3	26.6	
	30	37.4	33.1	30.3	
	45/315	37.8	(50.1)	(46.9)	53.4
	60	28.4	51.6	61.8	
	75	27.8	41.8	53.9	
3	90/270	29.1	39.0	44.9	42.9
	105	26.7	34.1	44.1	
	120	24.1	30.6	41.5	
	135/225	24.2	30.5	40.3	36.3
	150	25.2	32.8	41.2	
	165	25.7	35.9	42.6	
	180	27.6	38.4	43.8	44.1
	Average	28.1	35.6	42.1	39.8
	0/360	61.2	60.8	44.6	19.7
	15	66.3	62.1	50.1	
	30	71.3	63.1	54.7	
	45/315	69.9	68.9	60.9	56.9
	60	66.2	59.1	53.1	
1	75	52.9	46.6	49.7	
	90/270	42.4	41.3	42.6	44.4
	105	37.7	37.0	36.9	
	120	34.5	35.3	35.0	
	135/225	33.7	33.9	33.7	36.3
	150	33.1	32.7	33.2	
	165	31.5	32.0	31.4	
	180	31.1	39.2	30.7	31.5
	Average	48.6	47.1	42.8	37.8

( ) Data Pts differ by more than 20%

REDUCED HEAT TRANSFER DATA

Bundle Geometry - 4"-2DE

10"-bed solids loading 10"-grid to tube ℄ spacing

limestone bed - Blend B

Probe Row No.	Angular Position	Heat Transfer Coefficients (Btu/hr ft^2 °F) Superficial Velocity, FPS 3.9	8.1	11.9
5	0/360°	15.9	20.8	21.0
	45/315°	33.6	35.5	55.7
	90/270°	15.3	29.8	40.8
	135/225°	17.7	28.8	34.3
	180°	19.1	22.5	42.1
	Average	20.9	27.5	38.8
3	0/360°	19.9	28.7	23.5
	45/315°	27.9	(71.0)	60.6
	90/270°	21.2	56.0	60.1
	135/225°	19.8	49.7	53.8
	180°	18.8	52.2	50.2
	Average	21.5	51.5	49.6
1	0/360°	33.7	53.7	21.6
	45/315°	86.2	84.5	58.0
	90/270°	42.1	47.1	43.2
	135/225°	38.0	40.2	35.4
	180°	32.8	35.8	28.7
	Average	46.6	52.3	37.2

REDUCED HEAT TRANSFER DATA

Bundle Geometry - 4"-2DE

21" - bed solids loading 10" - grid to tube ℄ spacing

limestone bed - Blend B

Probe Row No.	Angular Position	Heat Transfer Coefficients (Btu/hr ft^2 °F) Superficial Velocity (FPS) 3.8	8.0
5	0/360°	23.5	24.1
	45/315°	50.7	45.2
	90/270°	20.1	48.2
	135/225°	20.2	37.1
	180°	23.2	40.8
	Average	27.5	39.1
3	0/360°	63.0	38.7
	45/315°	83.5	64.3
	90/270°	63.0	64.9
	135/225°	58.6	58.1
	180°	51.9	53.6
	Average	64.0	55.9
1	0/360°	57.7	44.7
	45/315°	60.7	63.3
	90/270°	38.2	40.0
	135/225°	33.1	33.7
	180°	28.9	29.5
	Average	43.7	42.2

REDUCED HEAT TRANSFER DATA

Bundle Geometry - 4"-2DE

18" - bed solids loading 18"-grid to tube ℄ spacing

limestone material - Blend D

Probe Row No.	Angular Position	Heat Transfer Coefficient (Btu/hr ft^2 °F) Superficial Velocity, FPS 4.0	6.2	7.96	9.9
5	0/360	17.3	16.0	16.6	58.2
	45/315	22.4	53.7	32.0	61.3
	90/270	21.6	28.4	31.2	37.0
	135/225	15.8	19.5	27.8	31.4
	180	15.0	19.7	31.8	37.6
	Average	18.4	27.5	27.9	45.1
3	0/360	17.3	19.5	19.7	16.4
	45/315	58.3	57.5	(50.1)	34.1
	90/270	33.7	35.7	40.3	36.4
	135/225	31.3	30.8	36.5	34.7
	180	37.2	35.7	40.7	36.6
	Average	35.6	35.8	37.5	31.6
1	0/360	47.6	40.1	21.5	16.2
	45/315	52.9	56.2	35.7	33.6
	90/270	44.3	40.9	45.7	37.9
	135/225	37.2	35.5	40.0	35.9
	180	35.9	33.8	39.3	34.9
	Average	43.6	41.3	36.4	31.7

( ) Data pts differ by more than 20%